University of Wollongong Theses Collection

University of Wollongong Theses Collection

University of Wollongong *Year* 2008

Dynamic bandwidth direct sequence - a novel cognitive solution for ultra-wideband communications

Jie Zhao
University of Wollongong

Zhao, Jie, Dynamic bandwidth direct sequence - a novel cognitive solution for ultra-wideband communications, ME-Res thesis, School of Electrical, Computer and Telecommunications Engineering, University of Wollongong, 2008. http://ro.uow.edu.au/theses/109

This paper is posted at Research Online.

http://ro.uow.edu.au/theses/109

NOTE

This online version of the thesis may have different page formatting and pagination from the paper copy held in the University of Wollongong Library.

UNIVERSITY OF WOLLONGONG

COPYRIGHT WARNING

You may print or download ONE copy of this document for the purpose of your own research or study. The University does not authorise you to copy, communicate or otherwise make available electronically to any other person any copyright material contained on this site. You are reminded of the following:

Copyright owners are entitled to take legal action against persons who infringe their copyright. A reproduction of material that is protected by copyright may be a copyright infringement. A court may impose penalties and award damages in relation to offences and infringements relating to copyright material. Higher penalties may apply, and higher damages may be awarded, for offences and infringements involving the conversion of material into digital or electronic form.

Dynamic Bandwidth Direct Sequence

– A Novel Cognitive Solution for Ultra-wideband Communications

A thesis submitted in fulfillment of the requirements
for the award of the degree

Master of Engineering Research

From

UNIVERSITY OF WOLLONGONG

By

Jie Zhao

Master of Engineering Studies

SCHOOL OF ELECTRICAL, COMPUTER

AND TELECOMMUNICATIONS ENGINEERING

2008

Statement of Originality

This is to certify that the work described in this thesis is entirely my own, except where due reference is made in the text.

No work in this thesis has been submitted for a degree to any other university or institution.

Signed

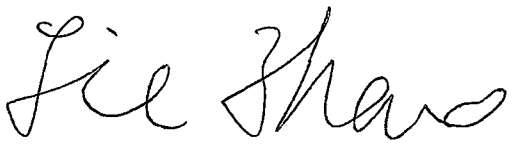

Jie Zhao

28 August, 2008

Table of Contents

Table of Figures

List of Abbreviations

ADC	Analog - digital converter
AWGN	Additive white Gaussian noise
BER	Bit error rate
BPSK	Binary phase shift keying
CP	Cyclic prefix
CR	Cognitive radio
DBDS	Dynamic bandwidth direct sequence
DS	Direct sequence
DVR	Digital video recorder
Eb/No	Ratio of Energy per bit to the noise spectral density
FCC	Federal communications commission
FFT	Fast Fourier transform
FH	Frequency hopping
HD	High definition
HDTV	High definition television
IFFT	Inverse fast Fourier transform
LAN	Local area network
MB-OFDM	Multiband orthogonal frequency division multiplexing
MCIDS	Multicode interleaved direct sequence
NBI	Narrow band interference
PAN	Personal area network
PN	Pseudo noise
RF	Radio frequency

SNR	Signal to noise ratio
TFC	Time frequency coding
TV	Television
UWB	Ultra-wideband
WAN	Wide area network
WLAN	Wireless local area network
WPAN	Wireless personal area network

Abstract

Ultra-wideband (UWB) Communication is currently considered as a key technology of the next generation wireless personal area network and wireless local area network. The use of very wide transmission bandwidth brings significant advantages in terms of high speed as well as low power transmission compared to traditional narrow band technologies. Ultra-wideband operation does not require a spectrum license but ultra-wideband devices are required to share spectrum with licensed narrow band users. As a concept to solve coexistence issues with other devices, cognitive radio used with ultra-wideband now becomes a new hot topic. Two mainstream development directions of ultra-wideband, MB-OFDM and DS based UWB, have all provided some cognitive solutions. However, both of them involve complicated computations such as IFFT/FFT and multiple pulse combination, not only increasing system complexity but also increasing manufacturing cost and power consumption.

This thesis presents a novel system for DS based UWB. The proposed dynamic bandwidth direct sequence (DBDS) system, focused on exploring a new idea rather than concentrating on impulse manipulation, provides a cognitive solution for DS based UWB in much simpler and more efficient way. Enhanced from the original MCIDS algorithm, this system is able to transfer data under a fraction of original spread spectrum signal bandwidth and different spectral shapes while maintaining the same data rate. This system does not require generating specific impulse for working environment, therefore significantly reduces system complexity. Different types of filters in the system enable a variety of potential transmission spectrums to satisfy

cognitive radio needs. This thesis also introduces a symbol combining mechanism over the original MCIDS to guarantee system performance under multipath channel.

Simulation results demonstrate that the DBDS has a very exciting performance. Even received with different bandwidths and different spectral shapes, the data information can still be fully recovered at the same data rate. The BER-Eb/No curve in ideal Gaussian channel exactly matches the theoretical curve, indicating that this system performs lossless with partial signal bandwidth. In multipath channel, the DBDS system still offers an excellent performance, incurring only a slight loss due to the cyclic prefix compared to the result in ideal Gaussian channel.

1 Introduction

1.1 Background

The exponential growth of wireless communication motivates the development of faster wireless devices not only for mobile or wide area network (WAN) but also for personal area network (PAN) and local area network (LAN). With the development of ultra-wideband (UWB), transmission capacity has been increasing either through direct sequence (DS based UWB) or multi-band orthogonal frequency division multiplexing (MB-OFDM). Ultra-wideband technology provides high speed yet low power transmission through the occupation of a wide spectrum. However, coexistence issue between multiple UWB devices or between UWB and narrow band devices is a serious challenge. This has led to the development of cognitive radio (CR) over UWB technology that allows spectrum sharing and interference suppression among UWB devices.

DS based UWB increases system performance over traditional impulse based UWB by using direct sequence spread spectrum technology, while maintaining a very simple system structure[1]. In DS based UWB, each pulse occupies a wide spectrum bandwidth. Current spectrum sharing and coexistence solutions over DS based UWB hence mainly focused on pulse shaping or how to generate a specific pulse that satisfies spectrum needs. Special pulse generation requires complicated algorithms, not only increasing system complexity but also being challenges for practical electronic circuits.

MB-OFDM has considered the issue of cognition from the very beginning of its design. This technology employs the concept of using traditional OFDM technology over multi-band. It can easily achieve spectrum sharing by simply turn off some transmit sub-bands that interferes with other devices. However, OFDM requires a large amount of processing such as FFT/IFFT that significantly increases system complexity as well as power consumption.

There is a considerable enhancement of DS based UWB technology to take advantage of the multi-code interleaved direct sequence (MCIDS) [2] technique. This thesis concentrates on the modification of MCIDS, in order to develop a new direct sequence based UWB system that achieves the cognitive radio advantage in a simple and efficient way.

1.2 Contributions

The contributions made in this thesis are listed below.

- Identified a common issue in current cognitive radio solutions for DS based UWB. Those solutions are mainly focused on how to generate a specific impulse that matches a spectrum hole. Most of impulse generation in those methods involves a large amount of signal processing, not only resulting in complicated structures but also requiring high standard electrical circuits to actually produce those impulses.

- Developed a simple and efficient mechanism to adjust transmission bandwidth for direct sequence technology without jeopardizing the transmission rate. Filtering a symbol sequence with different filters

according to the channel environment is the simplest way to adjust transmission bandwidth, but it cannot guarantee the correct recovery of the transmitted data information. Instead of reducing transmission rate as other traditional methods to avoid superimposition between chips, the new mechanism can keep the same data transfer speed. Even though each chip in transmitted sequence is spread into nearby chips, this mechanism can still fully recover signals because of the interleaved orthogonal codes employed in the algorithm.

- Extended concept of MCIDS to overcome multipath fading in reduced-bandwidth transmission. Multipath fading will degrade signal recovery in bandwidth-reduced MCIDS sequence, causing serious performance decrease. An enhanced method introduced in this thesis forces several MCIDS chips to experience the same amount of amplitude modification and fading in the filtering operation in multipath channel. As a result, transmission performance is only slightly reduced by the multipath effect.

- Proposed a new cognitive radio system called Dynamic Bandwidth Direct Sequence (DBDS) for use in direct sequence based ultra-wideband (DS based UWB). This system enables UWB device to transmit in half, a quarter, one eighth or even less of the original bandwidth but keeps the same data rate. Compared to the full bandwidth in traditional DS based UWB transmission, the occupied spectrum in DBDS system can be customized and dynamically allocated according to the changed channel conditions.

- Examined the system performance in both the ideal Gaussian channel and multipath fading channel. We show that in the ideal Gaussian channel, the DBDS system can be proven to be a lossless solution for cognitive radio UWB. In multipath fading channel, this system still provide excellent performance.

2 Literature Review

2.1 Introduction

This chapter introduces the current literature related to ultra-wideband and cognitive radio. Section 2.2 introduces the major ultra-wideband concepts, and Section 2.3 describes the history of ultra-wideband including theory and practical development over the last decades. Two major ultra-wideband technologies, direct sequence based UWB (DS based UWB) and multiband OFMD (MB-OFDM), are examined in Section 2.4. Section 2.5 includes potential UWB applications, followed by Section 2.6 that discusses cognitive radio over UWB including interference and coexistence issues. Section 2.7 summarizes the major advantages and disadvantages of DS-UWB and MB-OFDM in terms of achieving cognition.

2.2 Ultra-wideband (UWB) Concepts

2.2.1 Definition of Ultra-wideband

Ultra-wideband, defined by the federal communications commission (FCC), is any radio transmission technique that occupies a minimum of 500 MHz in spectrum or over 20 percent of fractional bandwidth, meanwhile satisfies the transmit power limits assigned by the FCC.

UWB offers many advantages over narrowband technology where certain applications are involved. Improved channel capacity is one major advantage of UWB. The channel is the RF spectrum within which information is transferred. Shannon's

capacity limit equation shows that the capacity increases as a function of BW (bandwidth) faster than as a function of SNR (signal to noise ratio):

$$C = BW * \log 2(1 + SNR) \tag{2.1}$$

where C = Channel Capacity (bits/sec)

BW = Channel Bandwidth (Hz)

SNR = Signal to noise ratio

and

SNR = P/(BW*No)

P = Received signal power

No = Noise power spectral density (watts/Hz).

Shannon's equation shows that increasing channel capacity requires linear increase in bandwidth while similar channel capacity increase would require exponential increase in power. This is why UWB technology is capable of transmitting very high data rates using very low power.

The key benefits of UWB can be summarized as

- High data rate.
- Low equipment cost.

The high data rate is perhaps the most compelling aspect from a user's point of view and also from a commercial manufacturer's position. The IEEE 802.11n draft standard can achieve a data rate around 108Mbps [3], but the extremely large bandwidth occupied by UWB gives itself the potential of even higher data rate that can enable new applications and devices that would not have been possible up until now.

The ability of transmission in very low power and without paying license fee for the occupied spectrum makes many manufacturers excited to build extremely cheap transceivers. This is possible by eliminating many of the components required for conventional sinusoidal transmitters and receivers.

2.2.2 Spectrum and Regulations

According to Title 47 of the Code of Federal Regulations (47 CFR), the bandwidth (−10 dB) of UWB communication devices is restricted within the 7.5 GHz of spectrum between 3.1 and 10.6 GHz.

The transmitter is the heart of the system, which consists of pulse generator and shaping circuitry and possibly additional output filter to produce the communications waveform. The regulation requires that any unintentional radiation emitted by the transmitter be investigated with respect to the power limits.

2.3 History of Ultra-wideband

The very fist ultra-wideband communication was employed by Guglielmo Marconi in 1901 [4] to transmit Morse code sequences across the Atlantic Ocean using spark gap radio transmitter. However the benefit of large bandwidth and relevant capabilities were never considered at that time.

Form 1960 to 1990, pulse based transmission – the early form of UWB, started to appear in high secure military communications such as impulse radar, automobile collision avoidance system and positioning system. In this period, the technology was

restricted to military and the Department of Defense of the U.S. Henning Harmuth, Gerald Ross, and K. W. Robins were the pioneers during those years. In late 1980s, pulse based transmission system was referred as carrier free baseband. In 1989, the term “ultra-wideband” was applied by the U.S. Department of Defense[4].

The U.S. government and other nation governments were also positively involved in UWB system development in this period for not only military but also commercial purposes. Many patents therefore were granted. In Leonard and Ross’s paper in 1978 [5], some examples of the use of UWB technology in radar and communications applications were presented, including collision avoidance systems, spacecraft docking, airport surface – traffic control, auto braking, ship docking, liquid – level sensing, and wireless communications.

Entering the twenty first century, UWB has evolved into two major technologies, one is extended from the orignal impluse based structure, called direct sequence ultra-widband (DS-UWB), mainly developed by Motorola and Freescale, and another is adopted from OFDM technology, called multiband OFDM (MB-OFDM), leaded by Intel croporation[6]. When Intel and its allies are working with local orgnizations worldwidely to permote its technology, other researchers and orgnizations support for DS-UWB, believeing that this techonogy is the optimal choice. Both of two technologies has been approved by FCC [7].

2.4 Mainstream Technologies of Ultra-wideband

There are two main solutions for UWB Communications

- Impulse radio or direct sequence based ultra-wideband (DS based UWB).
- Multiband orthogonal frequency division multiplexing (MB-OFDM).

2.4.1 DS based UWB

Technique Concepts

Original impulse radio UWB technology relies entirely on individual pulse that can be described as carrier free baseband impulse - it is able to operate without a carrier frequency. Originally, each pulse represents one bit of transmitted information directly, using PPM (pulse position modulation) and PAM (pulse amplitude modulation). Transmitted pulse waveform in DS based UWB is known as monocycle. One of the most commonly used monocycle pulses in DS-UWB systems is Gaussian monocycle. Other kind of pulses can also be employed in DS-UWB, such as orthogonal Hermite modified pulses. In general, each of these methods uses some forms of data modulation to insert data in the pulse [1]. A typical orthogonal Hermite pulse serial [8] used in UWB is shown in Figure 1 below.

In ultra-wideband, the flatter and lower power spectral density (PSD) the signal can provide, the less likely that narrowband transmission can be interfered. However, the commonly used signals in early UWB generated by time-hopping and pulse position modulation demonstrate a lot of spectral peaks [9]. This often causes argument regarding the application of UWB technology. Later in 2001, Huang and Li [10]

proposed direct sequence spreading of the data using long PN sequence with extremely narrow chips. For biphase modulation, the generated UWB signal can be written as

$$s(t) = \sum_{j=-\infty}^{\infty} w(t - jT_c) c_j \, d_{\lfloor j/N_s \rfloor} \tag{2.2}$$

where $d_{\lfloor j/N_s \rfloor}$ is the $\lfloor j/N_s \rfloor th$ data bit, c_j is the *j*th chip of the pseudorandom code and the *w(t)* is the pulse waveform. N_s represents the number of pulses to be used per data bit, T_c is the chip length and T_d is the bit length. By the use of this period extension technique, considerable reduction in the power spectral density level can be obtained, and also the generated near-white spectrum UWB signal provides less interference towards narrow band devices.

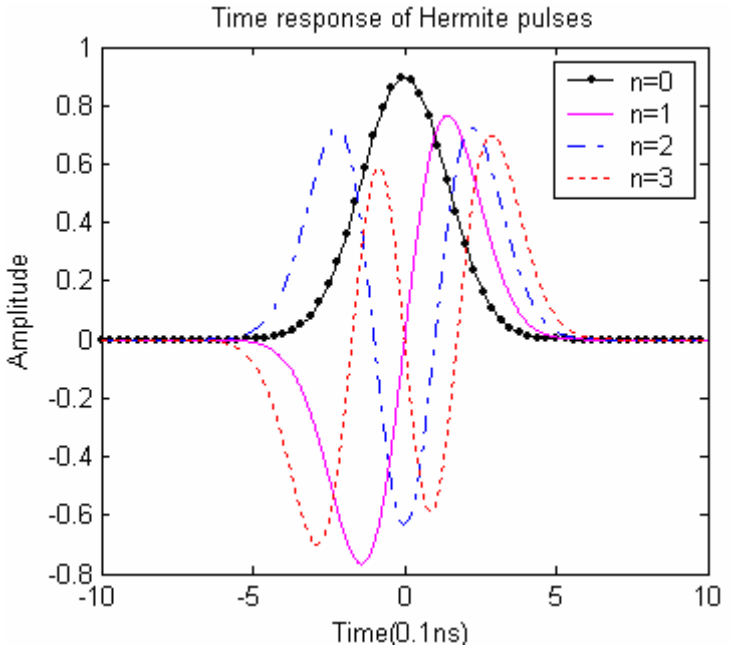

Figure 1. Examples of orthogonal Hermite pulse in four orders.

In the receiver end, the transmitted UWB signal will be detected simply by the periodic autocorrelation function of the original PN sequence. Figure 2 illustrates the

structure of the DS-UWB transmitter[11].

Properties

The significant benefits of DS based UWB are:

- Simple structure
- Low power requirement
- Low production cost
- Enables distance detection and positioning among two DS based UWB devices [12][13].

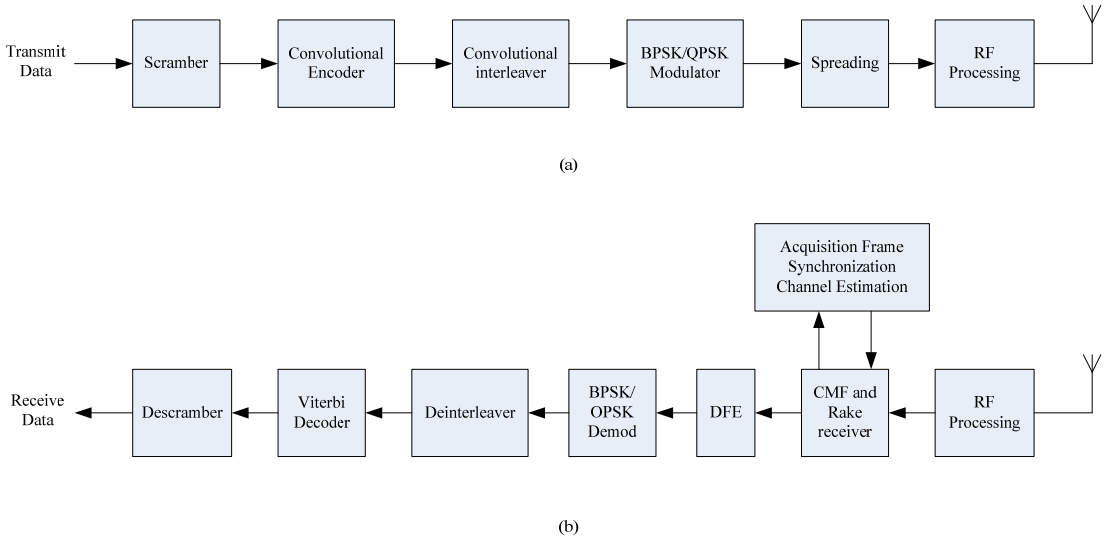

Figure 2. Block diagram of the DS-UWB transceiver. (a) transmitter. (b) receiver.

The main disadvantages of these systems are:

- The ISI can severely degrade the performance, since the spreading factor is relatively small for high data rates as compared with that of traditional DS based system. This necessitates an equalizer at the receiver [11].
- The challenge of building RF and analog circuits with large bandwidths, high

speed analog-to-digital converters (ADCs) to process this extremely wideband signal, and the significant digital complexity required to capture the multipath energy in dense multipath environments [14].

- DS based UWB may be immune to certain amount of NBI, but still might interfere low power local narrow band devices or be interfered if the transmission power is large enough.

2.4.2 Multiband OFDM

Technique Concepts

MB-OFDM provides a solution to the multipath energy collection issue by combining orthogonal frequency division multiplexing (OFDM) system with multi-banding. The time-frequency coding (TFC) is performed across OFDM symbols. That is, the transmit signal hops over different sub-bands every OFDM symbol duration. Figure 3 shows an example of how the OFDM symbols are transmitted in an MB-OFDM system [14].

In this example, only three groups of band are used for simplicity, while in practice, however, more groups are used. Each band group is composed of either two or three separate sub-bands. In the system, a guard interval is appended to each OFDM symbol and a zero-padded prefix is inserted at the beginning of each OFDM symbol. The guard interval ensures that there is sufficient time for the transmitter and receiver to switch to the next carrier frequency. A zero padded prefix provides both robustness against multipath and eliminates the need for power back-off at the transmitter. The whole structure of MB-OFDM is illustrated in Figure 4[11].

Properties

MB-OFDM provides abilities such as:

- It efficiently captures multipath energy with a single RF chain, insensitivity to group delay variations [15].
- It deals with narrowband interferers at the receiver without having to sacrifice either sub-bands or data rate [15].
- It offers simplified synthesizer architectures and relaxes the band-switching timing requirement.

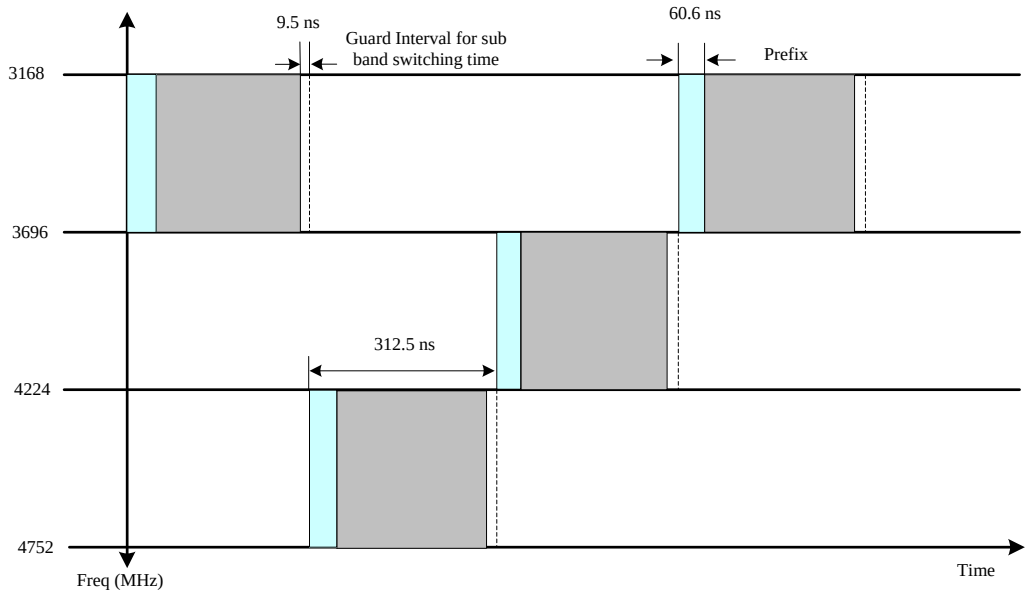

Figure 3. Example of TF coding for an MB-OFDM system [9].

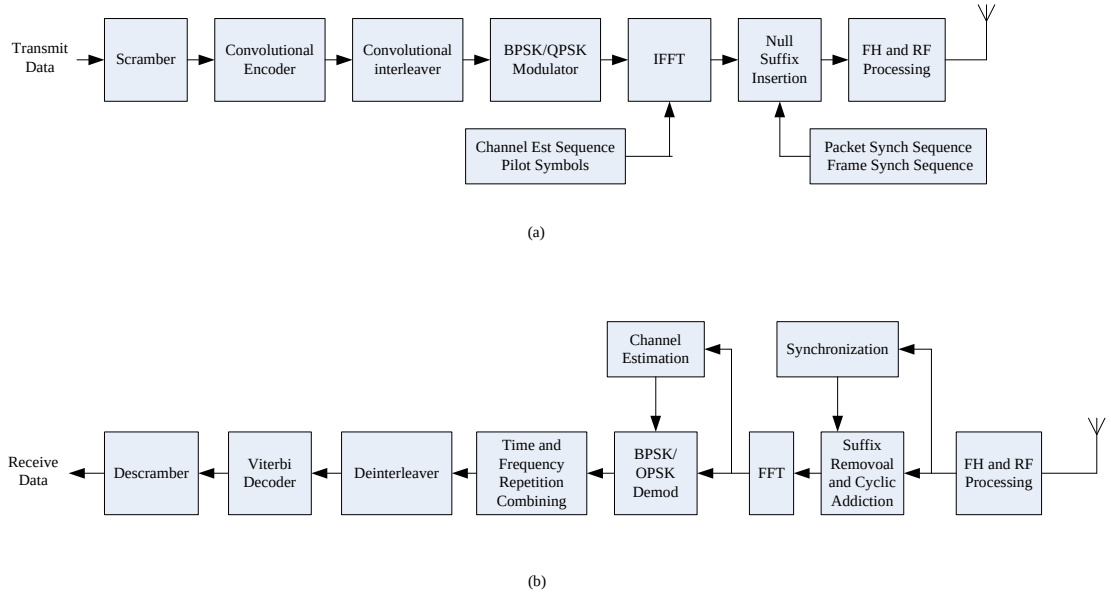

Figure 4. Block diagram of the MD-OFDM transceiver, (a) transmitter. (b) receiver.

The main disadvantage can be listed as:

- Complicated transmitter due to the Fast Fourier Transform mechanism and higher peak-to-average ratio than DS-UWB[14].
- Requirement for relatively large computational power because of the needed FFT[16].
- Lack of the ability to detect distance as DS-based UWB does.

2.5 UWB Applications

2.5.1 Consumer Electronics Devices

Because UWB is capable of handling multiple streams of digital audio/video and multiple HDTV streams with a quality level equivalent to a wired system at short ranges, many UWB applications are focused on multimedia streaming. Potential applications include the transfer of digital content between devices in different

entertainment and computing clusters at home, such as DVR, set-top boxes, digital TV broadcasting, HD Flat-Panel Displays, Game Consoles and PC accessories. Consumer wireless entertainment is viewed as the first large growth area for ultra-wideband technology, making up a great percent of the total UWB unit shipments.

UWB is the only wireless technology that is capable of handling multiple streams of digital video, such as HDTV streams [17]. This will become increasingly important as the industry shifts to HDTV, Blue Ray disc and H.264 format over the next few years when consumers demand wireless products to keep their home entertainment systems uncluttered and easily reconfigured/repositioned. Wireless displays will also be a key target market, especially as consumers continue to demand larger displayers.

2.5.2 UWB for PC-oriented Applications

UWB has much to offer for PC networking as a complement to Wi-Fi because of its ad hoc and quality-of-service qualities needed for media and peripherals. While UWB will appear first in the home for wireless PAN applications, we believe it will find its way into corporate networks as well as home networks over the next few years in laptop, desktop computers and printers. Eventually, UWB will be also likely used in next-generation access point and switches/routers.

Wireless Personal Area Networks

UWB will start out as wireless PAN multimedia-focused solution and penetrate the home networking market first. The trade-offs between power consumption, data rate,

and range have also kept most UWB developers focused on shorter ranges in order to comply with current FCC rules while providing very high bit rates[18],[19] and [20].

Wireless Local Area Networks

While most of the initial market focus will be on wireless PAN applications there is no reason why UWB cannot or will not be used for longer-range applications as well. It is important to remember that UWB is a physical layer technology, which makes it a likely PHY for future Wi-Fi standards such as 802.11n, which supports a data rate at 108Mbps. Initial target markets for theses UWB-based WLAN chip sets are airports as well as homeland security applications. The unique advantages of UWB for wireless LANs include:

- Large data rate and payload capacities for WLAN applications than existing Wi-Fi or alternative UWB WPAN-only solutions
- Enhanced security
- Positioning capabilities
- Signal coexistence with other RF technologies

2.5.3 UWB for Other Applications

UWB also has many other applications. Since the beginning of invention, UWB has been used in US military as a radar technology [21],[22] and [23], providing high secure, low power, light weight services.

UWB can also take part in the next generation mobile communication. Under the consumer requirement of higher speed and lower cost, the fourth generation (4G)

mobile communication is wildly previewed as a revolution from cell phone into modular multi-radio, multi-application platform. The role of UWB in this platform is set to be a medium mobility, high speed terminal [24],[25],[26] and [27].

The low power consumption makes UWB a great choice for high speed battery operated wireless applications [28], such as the use in smart sensor network [29].

2.6 Cognitive UWB Radio

2.6.1 Need of Cognition

Radio spectra are limited natural resources. In response of the increasing demand for wireless connectivity and current crowding of spectrum utilization, FCC has regulated the usage of radio spectrum and radio power emission based on specific band assignments designated for a particular service. From the spectrum allocation by FCC [30], it is easy to find out that current wireless channel is extremely crowded. Almost all the available bands have been utilized and licensed. Once the frequency bands are allocated, they are assigned the complete rights to a primary user, and therefore it is extremely difficult to be recycled, no matter how inefficiently those users utilize them. However, as we know that UWB must utilize a wide bandwidth from 3.1 GHz to 10.6 GHz, the overlapping with existing and planned narrowband radio systems in this spectrum range is unavoidable. In this case, UWB transmission must be suspended to protect licensed users unless a solution is proposed.

On the other hand, UWB itself faces its own problem. Even though UWB systems have inherent immunity to certain amount of narrow band interference (NBI), due to the low power spectral density, a significant performance loss is possible when the NBI is of sufficient power such as IEEE 802.11a device operating nearby [31, 32]. It seems that the need for coexistence and compatibility between UWB and narrowband wireless devices has become a key issue that must be solved.

One way to overcome the interference challenge is to work on the usage over spectrum. The fact is, although the spectrum chart seems to indicate a high degree of spectrum utilization, the actual spectrum utilization is very low. Some frequency bands are largely unoccupied most of the time, or are only partially occupied [33]. The usage of allocated spectrum below 3 GHz band is only from 15% to 85%, typical channel occupancy was less than 15% [34]. To increase utilization efficiency, a highly successful experience in ISM (2.4GHz) band and UNII (5-6GHz) and microwave bands can be adapted – making spectra available on an unlicensed basis. By this concept, secondary users are allowed to share the same spectrum with primary users under the requirement that they limit their interference to pre-existing primary users.

Meanwhile, research indicates a coexistence limitation between UWB devices. This problem is even more serious and practical than interference issues between UWB and narrowband devices [35]. This problem is also worth paying attention to.

2.6.2 Cognitive Radio Concepts

Cognitive radio, a spectrum sharing concept, was introduced by Mitola [36] as a solution for the spectrum sharing challenge. The term “cognitive radio”, can formally be defined as follows: cognitive radio is a paradigm for wireless communication in which either a network or a wireless node changes its transmission or reception parameters to communicate efficiently avoiding interference with licensed or unlicensed users. The basic operating principle of cognitive radio [37] is the ability to sense whether a particular band is being used or not. If not, then CR utilizes the spectrum without interfering with the transmission of other authorized users. If the primary user of a band recommences transmission, the radio jumps to another band, or stays in the same band, altering its transmission or modulation scheme to avoid interference.

Cognitive radio has the potential to provide a number of benefits that would result in increased access to spectrum and also make new and improved communication services available to the public. Cognitive radio provides several capacities that allow for more efficient, flexible spectrum use including [38]:

- Frequency Agility – the ability of a radio to change its operating frequency to optimize use under certain conditions.

- Dynamic Frequency Selection – the ability to sense signals from other nearby transmitters in an effort to choose an optimal operating environment.

- Transmit Power Control – to permit transmission at full power limits when necessary, but constrain the transmitter power to a lower level to allow greater sharing of spectrum when higher power operation is not necessary.

- Location Awareness – the ability for a device to determine its location and the location of other transmitters, and first determine whether it is permissible to transmit at all, then to select the appropriate parameters such as the power and frequency allowed at its location.

- Negotiated Use – A CR could incorporate a mechanism that would enable sharing of spectrum under the terms of a prearranged agreement between a licensee and a third party. Cognitive radios may eventually enable parties to negotiate for spectrum use on an ad hoc or real-time basis, without the need for prior agreements between all parties.

2.6.3 Implementing Cognitive Radio on UWB

Through many years of development, ultra-wideband now can provide several capabilities that satisfy the requirements of cognitive radio. Seven main features of UWB that suit for cognitive radio including [39]:

- Limited interference to licensed systems.
- Adjustable data rate and quality of service.
- Adaptable transmit power.
- Adaptive multiple access.
- Information security.

- Limited cost and complexity.

Those features are mainly contributed by four methods, which are investigated in the rest of this section.

1. Power control

Cognitive radios aim at an opportunistic usage of licensed frequency bands under the condition that the interference caused by cognitive devices to licensed users remains at negligible level.

UWB offers the possibility of being implemented in two basic approaches – underlay mode and overlay mode [40]. Underlay mode is approached with severe restrictions on transmitted power level with a requirement to operate “ultra” wide bandwidth. In this mode, it complies with the FCC regulations in the USA and is almost impossible to affect existing licensed system[41]. Alternatively, the overlay mode is based on avoidance of higher priority users through the use of spectrum sensing and adaptive allocation. In this mode, the transmitted power can be much higher but the bandwidth is limited. However, this mode is only applicable if the UWB transmitter ensures that the targeted spectrum is completely free of signals from other systems, and if the regulations allow this mode of operation. When these two conditions are met, UWB transmission power can be increased to a comparative level as much of the licensed user. Underlay and overlay mode are shown in Figure 5.

UWB can operate under both modes, or switch between them depending on the spectrum vacancy. When spectrum meets the overlay mode requirement, UWB can

immediately increase its transmit power and work in overlay mode. Also UWB signal can be shaped in a way that part of the spectrum is occupied in an overlay mode, while some other parts are occupied in an underlay mode. These operations enable UWB to cause negligible interference to other narrowband systems.

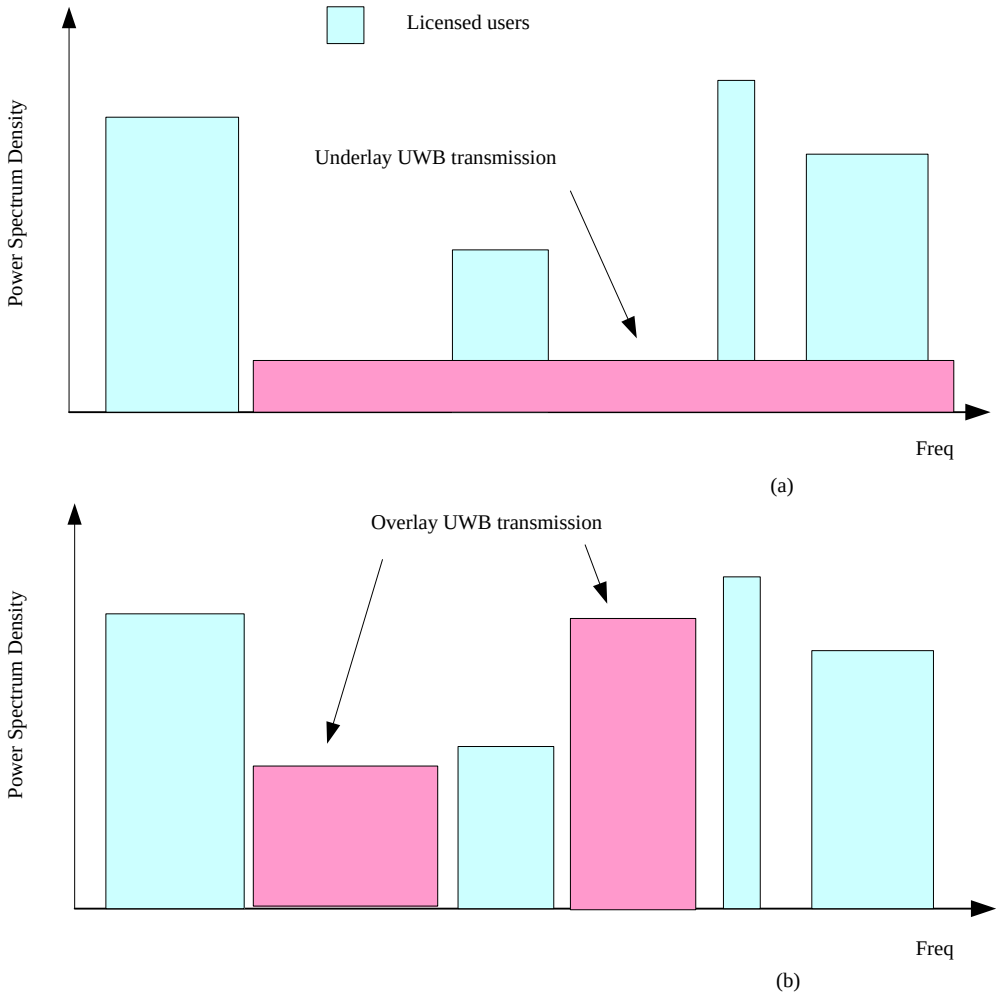

Figure 5. (a) Underlay mode and (b) overlay mode of UWB spectrum sharing with primary users.

2. Multi-carrier system

Cognitive radio is expected to have a high flexibility in determining the spectrum it occupies. MB-OFDM has developed a way of spectrum shaping through its nature multiple carriers.

In OFDM, tones are placed at regular frequency interval to avoid the inter-carrier interference. Each tone occupies 4.125 MHz, and this bandwidth is reasonably fine-grained to craft a notch without excessively sacrificing the system throughput [42]. MB-OFDM has the ability to detect interference levels in specific victim receiver bands via the FFT engine. By using OFDM, the transmitted spectrum can be easily shaped so as not to inject harmful interference. By using FFT, the MB-OFDM device can approximate a spectrum analyzer that detects average power level that transmitted within MB-OFDM band range. Based on the information sensed, spectrum shaping can be conveniently accomplished by turning some sub-carriers on or off according to the spectral condition [43, 44]. This behavior is called inserting a notch.

An MB-OFDM device can insert a notch into the spectrum using one of the following techniques[43]: (1) zero tones within and on either side of the victim receiver band, or (2) zero tones within the victim receiver band and use data-specific tones on either side of the band in order to sharpen the notch edges. Typically, the first approach requires a large number of zero tones adjacent to the victim receiver band in order to create a deep notch, but the implementation is extremely simple and the receiver requires no a priori knowledge of which tones have been zeroed. On the other hand, the same notch depth can be obtained via the second approach using fewer tones. This

approach is more complicated to implement and requires the receiver to have a priori knowledge of the tone locations that have data-specific values.

3. Antenna design

Some researchers developed some antenna designs. Proposed antennas vary at shape, material, and even ports [27],[45]. Those antennas can filter out certain signal band and isolate other unwanted frequency. Some of it can even support dual band to receive both narrow band WLAN signal and UWB signal at the same time[46]. However those antennas only support specific applications, not able to cognitively receive different bands according to the channel environment.

4. Pulse shaping

In DS based UWB system, since the communication is basically realized via the transmission of short pulses, varying the duration or the form of the pulses can directly alter the occupied spectrum. Therefore, the flexible and adaptive pulse waveform design is essential in order to provide an appropriate radio solution to maintain coexistence and interoperability among various existing or forthcoming narrowband as well as UWB systems.

At present, DS based UWB aims at designing a number of adaptive pulse waveforms corresponding to required spectrum notches for cognitive coexistence with interference avoidance. This kind of adaptive pulse waveforms is preferred to be expressed by a limited linear combination of core pulse shapes namely orthogonal basis functions and related auxiliary functions or factors. These core pulse shapes (i.e. basis functions) are expected to posses the following properties [47].

- The basis function's spectrum should be contained in a desired frequency sub-band allocated by the FCC spectral mask, namely being bandwidth-limited.

- The basis function's waveform should be limited to a short duration with an efficient energy concentration, realizing data rate as high as possible and inter-pulse-interference as low as possible, namely being time-limited.
- These basis functions are preferred to be orthogonal with each other, so as to allow for a linear combination of them for further designing much more complex pulse waveforms as needed.

- The basis function set, if preferred, is flexibly combined or extended, being capable of fitting any further wireless channel change as well as spectral mask modification by other regional regulatory committee around the world.

A set of pulse designs based on the above properties can be found through the recent years. A frequency coded orthogonal UWB pulse is explained in [48]. Based on orthogonal carriers and PN codes, by choosing proper original pulse and the PN code, their pulse can be deployed to comply with the FCC spectral mask. In an example of avoiding WLAN interference at 5.8 GHz, this technology produces about -50dB notch.

Meanwhile in Zhang's work [49], a pulse series based UWB CR system is proposed for narrow band interference (NBI) suppression. In their proposed scheme, the waveform is linearly composed by series of same pulses. Those basic waveforms can be any waveform that satisfies the FCC's spectrum limitation.

Similar methods of designing pulses can also be found in [50], [51], [52] and [53]. Among all those pulse shaping technologies, every design can suppress the NBI effectively. However, due to the employment of long duration transmission waveform for each bit, pulse shaping scheme may decrease data rate while performing interference suppression. Meanwhile, generation of those pulses involves large amount of calculation, which will definitely increase power consumption. Also, generating those complex shaped waveforms needs high clock timer, which is still a great challenge for current analogue circuits.

2.7 Chapter Summary

Direct sequence based UWB and MB-OFDM are two major technologies in the UWB area. Both of them have found a certain amount of applications. DS based UWB has a simpler structure and lower cost, which makes it easier to be accepted by consumer market. MB-OFDM employs IFFT calculation, which leads to a complicated structure and higher cost. To deal with the challenge of cognitive radio, MB-OFDM can simply turn off some of its sub-bands that interfere with other devices because of its OFDM nature. On the other hand, more complicated techniques have to be developed for DS based UWB system to achieve cognition. Most of the cognitive DS UWB systems focus on how to generate a specific pulse that satisfies cognition needs. However, this type of method requires a large number of calculation as well as high power consumption. Also this method can be a potential challenge to hardware design.

3 System Model of Dynamic Bandwidth Direct Sequence

Most research of cognitive radio on DS based UWB has focused on how to generate an UWB pulse to match the FCC spectral mask. Alternatively, a dynamic bandwidth Direct Sequence is proposed in this thesis to extend and modify traditional multicode interleaved direct sequence (MCIDS) algorithm, which provides a solution to enable receiving and fully recovering user data from part of the transmitted signal bandwidth without necessarily decreasing data rate. The adjusted bandwidth can be a half, one fourth, one eighth or even less of the original bandwidth. This new algorithm can be implemented easily and it only slightly increases system complexity. Therefore, this technology provides an opportunity for cognitive UWB transmission in a very simple and efficient way.

The rest of this chapter is organized as follows. The fundamental concepts, traditional MCIDS, CP and spectrum adjusting are introduced in section 3.1, 3.2 and 3.2. Section 3.4 describes the detailed system model, including a demonstration of how each block works.

3.1 Multicode Interleaved Direct Sequence (MCIDS)

Original MCIDS [2] spreads a signal block of N data bits into a long interleaved sequence to suppress inter-symbol interference (ISI). An example of MCIDS spreading is presented in Figure 6 [54], where (*a*) shows the spread signal obtained

by spreading symbol +1 with its corresponding spreading code $\{+1,+1,\ldots+1\}$, (b) shows the spread signal obtained by spreading signal with its corresponding spreading code $\{-1,+1,\ldots-1\}$ and (c) is obtained in the same way. Afterwards a block interleaver then outputs data as $\{a_0,b_0,c_0\ldots a_1,b_1,c_1\ldots a_{N-1},b_{N-1},c_{N-1}\ldots\}$ shown in (d). A length P_0 cyclic prefix (CP) is also added in this example, which is the same as the last segment of the block interleaved signal.

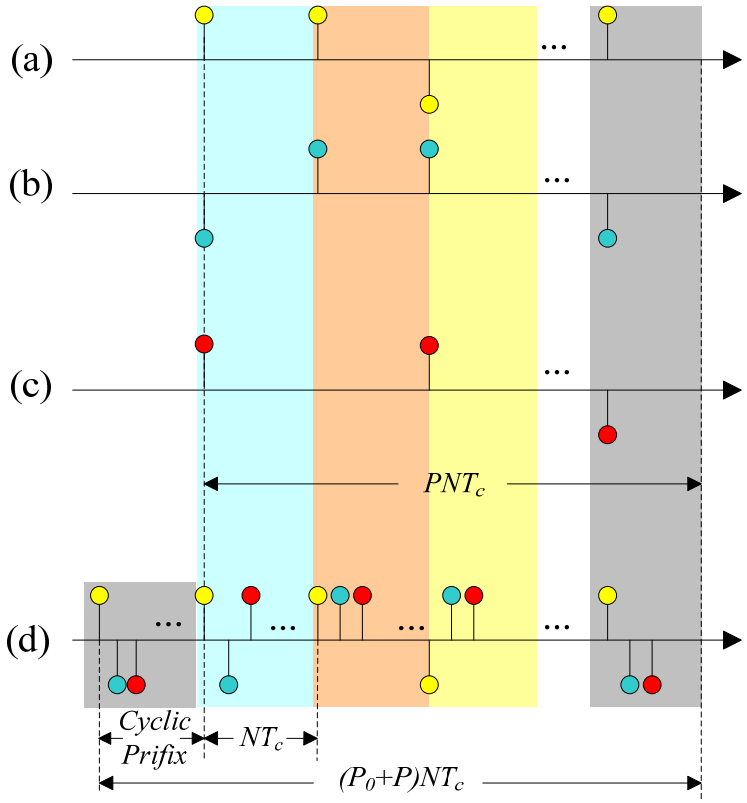

Figure 6. An example of MCIDS spreading.

3.2 Cyclic Prefix for ISI Suppression

Cyclic prefix in MCIDS system as well as the proposed system is an important component to suppress the effect of multipath. Figure 7 explains how the CP works.

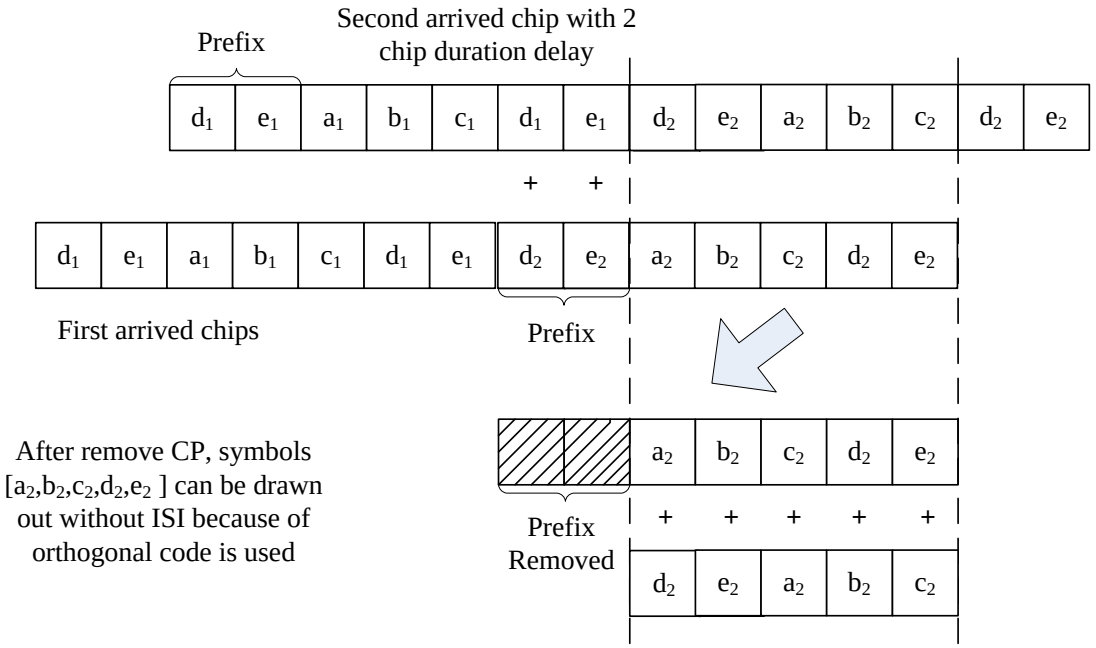

Figure 7. Illustration of ISI suppression by CP.

In Figure 7, two frames of chip, $\{d_1, e_1, a_1, b_1, c_1, d_1, e_1\}$ and $\{d_2, e_2, a_2, b_2, c_2, d_2, e_2\}$ are used as example, where d_1, e_1 and d_2, e_2 in the beginning of each group are the prefix belonging to its group. We assume that the first vector from path 1 arrives at receiver antenna with 2 chip duration delay, and the second vector from path 0 arrives with no delay. In this scenario, the last two chips in the first group, d_1, e_1, will arrive at the same time as the first two chips of the second group, d_2, e_2, However, due to the fact that chip d_2, e_2 in the beginning of frame 2 are just repeat of the last 2 chips in this frame, they can be simply wiped from this frame. The rest in received frame contains only information of frame 2. Therefore, chips in frame 2 would not be interfered by frame 1, and thus the ISI is eliminated.

3.3 Spectrum Adjusting Over MCIDS

In the proposed system, impulse duration can be controlled by customized filter with bandwidth $|f| = 2^{-m}\frac{1}{T_c}$, where $m = 0,1,2\ldots$. The filter can be low pass, high pass, band pass, or band stop filter depending on channel spectrum hole. The simple fact is, decreasing the bandwidth of every single impulse to 2^m times lower, in other word, to 2^{-m} of original, will also means increasing its duration to 2^m longer than original. This operation leads to overlapping of successive impulses. Note that the limited bandwidth must be exactly 2^{-m} times of the original bandwidth to facilitate further processing. Taking $m = 0,1,2$ for example, after spectral shaping and matched filtering, each impulse is reshaped in the time domain as illustrated in Figure 8.

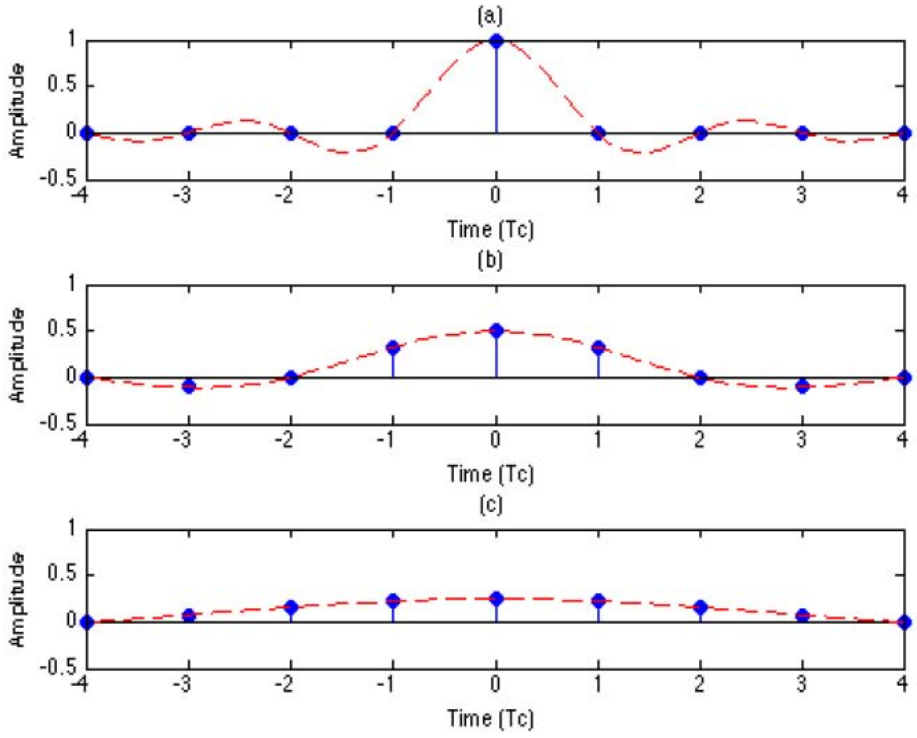

Figure 8. Example of filtered impulses, (a) m = 0, with full bandwidth, (b) m =1, impulse with half bandwidth (c) m =2, impulse with quarter bandwidth.

In Figure 8, when $m = 0$, at the sampling points, no ISI is produced since the impulse is zero at integer multiples of T_c. The MCIDS signals are fully passed in the frequency domain. This condition can be considered as that of the unfiltered MCIDS signal, and signal processing can be performed in the traditional way as in [54]. When $m = 1$, however, signal bandwidth is reduced to half of the original bandwidth. Each input impulse has nonzero amplitudes at integer multiples of T_c. When $m = 2$, signal bandwidth is reduced to quarter of the original bandwidth. In other words, when impulse is filtered, each output impulse sample is a contribution of several impulses. This overlapping effect is shown in Figure 9.

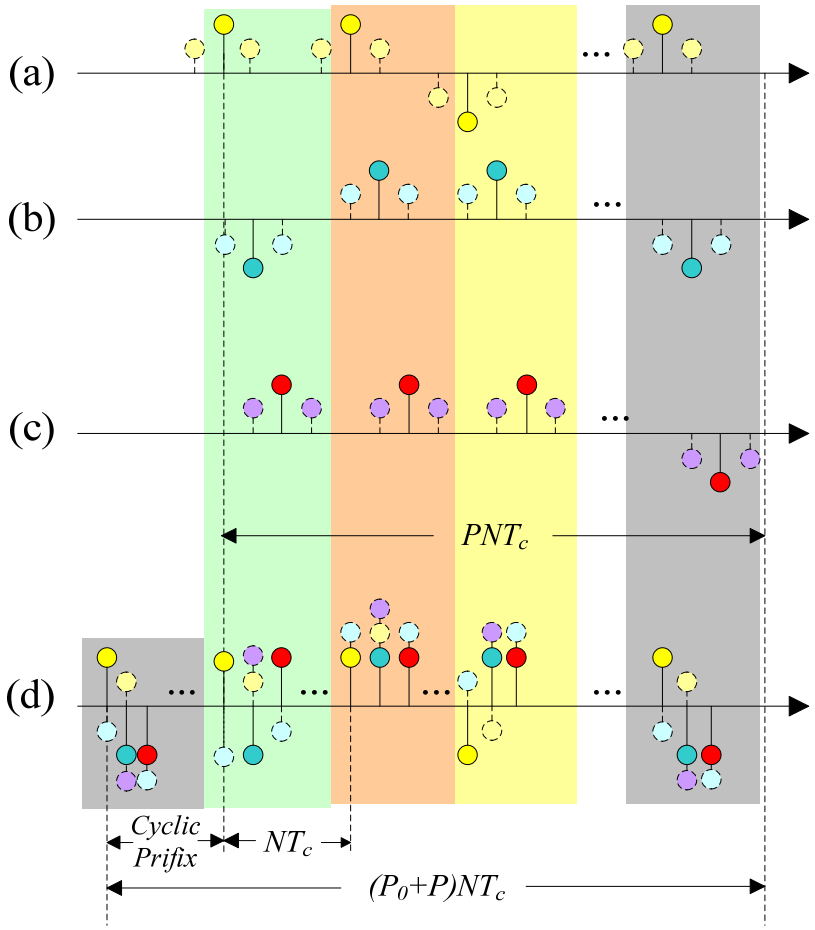

Figure 9. Spectral shaped signal sequence.

3.4 System Model

The new dynamic bandwidth direct sequence (DBDS) system is an evolution over the original MCIDS technology. This new system enables signal recovery from part of the original bandwidth of the MCIDS system by using a wider signal impulse in the time domain. The general system model can be described as in Figure 10.

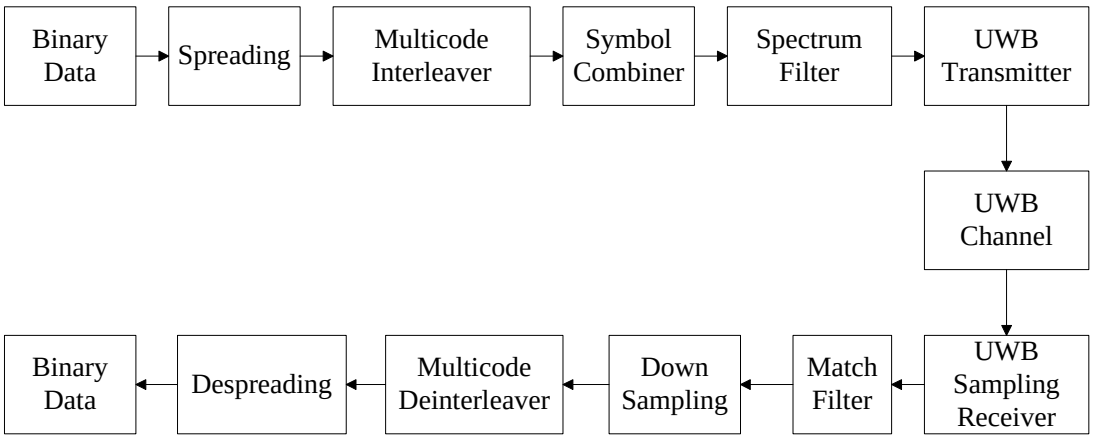

Figure 10. Block diagram of equivalent system model.

In this proposed system, the transmitter end is formed by four main blocks, including direct spreading, multicode interleaving, symbol combining and bandwidth adjusting. The receiver end of the system contains a few more steps, which are matched filtering, down sampling, multicode deinterleaving, despreading, channel equalization and signal detection. Detailed functions of each block are described below:

- Spreading

This block spreads encoded user data at a relatively low rate over a much wider bandwidth using a sequence of pseudorandom units called chips at a much higher rate.

By assigning a unique code to each bit, the receiver, which has knowledge of the code of each bit, can successfully separate the desired signal from the received waveform. The orthogonal code can be chosen from a wide range of orthogonal code sets, such as Hadamard code, Walsh code, orthogonal variable spreading factor (OVSF) code, etc. However, the system bit error rate may vary depending on the orthogonality (auto correlation and cross correlation performance) of the chosen code.

The code generator periodically produces orthogonal codes for each bit of user data. If the code set has a length of P, which means P different orthogonal codes, each code will have a period of P in the same time. In the spreading operation, the first user data bit correlates with the first code, the second bit with the second code, until the P th bit correlates with the $P\,th$ code. Then $P+1\,th$ bit correlates with the first code, to start another loop. Therefore totally P^2 chips are produced in every spreading loop. An example of this operation is shown in below:

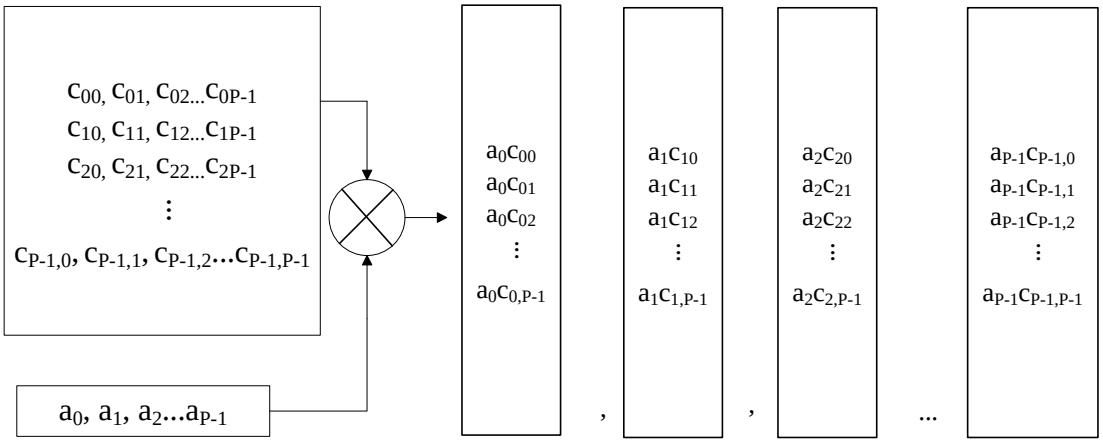

Figure 11. One loop of spreading spectrum.

In Figure 11, $a_0, a_1, a_2, \ldots a_{P-1}$ is one group of user data, and c_{00} to $c_{0,P-1}$, as well as other rows of $c_{i,j}$, are P rows of the orthogonal codes.

- Multicode interleaver

This block performs multicode interleaving operation and insert cyclic prefix (CP) for every P chips after a spreading loop is done. Chips produced from spreading will be stored in buffer matrix until P^2 chips are collected. In the interleaving operation, this block fills those chips into a $P \times P$ matrix in row wise. To insert CP, simply add the last P_0 rows above to the first row. An example of this matrix is shown below.

$$
\begin{array}{l}
\left.\begin{array}{l} \\ \\ \\ \end{array}\right\} P_0 \text{ rows of CP} \\
\left.\begin{array}{l} \\ \\ \\ \\ \end{array}\right\} P \text{ rows}
\end{array}
\begin{bmatrix}
a_{P-P_0-1}c_{P-P_0-1,0} & a_{P-P_0-1}c_{P-P_0-1,1} & a_{P-P_0-1}c_{P-P_0-1,2} & \cdots & a_{P-P_0-1}c_{P-P_0-1,P-1} \\
\vdots & \vdots & \vdots & \cdots & \vdots \\
a_{P-2}c_{P-2,0} & a_{P-2}c_{P-2,1} & a_{P-2}c_{P-2,2} & \ddots & a_{P-2}c_{P-2,P-1} \\
a_{P-1}c_{P-1,0} & a_{P-1}c_{P-1,1} & a_{P-1}c_{P-1,2} & \cdots & a_{P-1}c_{P-1,P-1} \\
a_0c_{0,0} & a_0c_{0,1} & a_0c_{0,2} & \cdots & a_0c_{0,P-1} \\
a_1c_{1,0} & a_1c_{1,1} & a_1c_{1,2} & \cdots & a_1c_{1,P-1} \\
\vdots & \vdots & \vdots & \ddots & \vdots \\
a_{P-2}c_{P-2,0} & a_{P-2}c_{P-2,1} & a_{P-2}c_{P-2,2} & \cdots & a_{P-2}c_{P-2,P-1} \\
a_{P-1}c_{P-1,0} & a_{P-1}c_{P-1,1} & a_{P-1}c_{P-1,2} & \cdots & a_{P-1}c_{P-1,P-1}
\end{bmatrix}
$$

Figure 12. $\left(P_0 + P\right) \times P$ **sized buffer matrix row-wisely filled by chips and CP.**

- Symbol combiner

This combiner does its operation in the buffer matrix too. The combining operation row wisely merges the elements of every 2^m row into one row, but remains the same matrix size. The elements in the first of every those 2^m rows is replaced by the sum of all 2^m rows, and the rest elements are set to zero.

Chips in this matrix are then output in column wise. The total number of chips is $P\times(P_0+P)$. To explain in a simple way, if the original MCIDS leads to an output in the form of

$$\{a_0,b_0,c_0\ldots a_1,b_1,c_1\ldots a_{N-1},b_{N-1},c_{N-1}\ldots\}.$$

Then the output after the combining block then would be in the form of

$$\{(a_0+b_0+c_0+\ldots),0,0,\ldots,(a_1+b_1+c_1+\ldots),0,0,\ldots,(a_2+b_2+c_2+\ldots),0,0,\ldots,\}.$$

Different from the original MCIDS in Figure 6, the output chips in time domain can be illustrated as Figure 13.

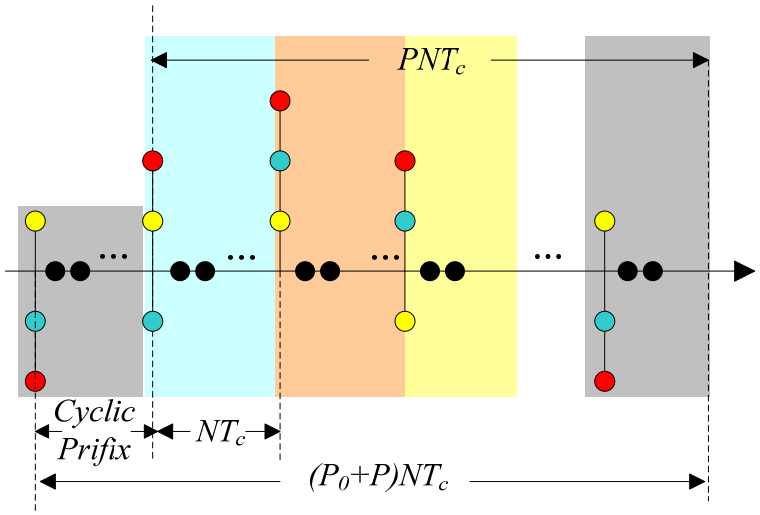

Figure 13. Every 2^m chips are added into one chip, while others are set to zero.

.

- Bandwidth adjusting filter and matched filter

These two blocks together shape the spectrum of the chips and adjust its bandwidth by using a digital filter. Based on the wireless channel environment and cognition requirement, various filters employed in this block can be chosen from high pass, low pass, band pass or band block filters. The adjusted bandwidth, however, must be limited to 2^{-m} of the original bandwidth, such as $\frac{1}{2},\frac{1}{4},\frac{1}{8}$, etc. After the bandwidth

adjustment, in Figure 13, chip duration is lengthened and therefore causes overlapping, similar to the cases shown in Figure 8. Through this operation, signals contained in each chip will be spread into nearby chips. In other word, each chip after bandwidth adjusting will contain not only information of itself, but also information of nearby 2^m chips. However, due to the orthogonality of the spreading code, bit information corresponding to specific spreading code would still be able to recover from the overlapped signal in despreading operation. The algorithm of this signal recovering will be explained in the next chapter.

- Down sampling multicode deinterleaver

At the receiver end, the multicode deinterleaver operates exactly in the reverse order of the interleaver. Interleaved chips are also column-wisely filled into $\left(N+P_0\right)\times P$ matrix. Then, all the P_0 rows of CP are removed to suppress ISI from different vector.

As the final step, the chips in matrix are down sampled at rate 2^m. At the receiver end, since information is overlapped from one chip into nearby 2^m chips, only one in every 2^m chips are required for down sampling. Note that in the multipath channel, signals from different path may overlap onto the next couple of chips. Therefore in this situation, the same data can also be collected from the next couple of chips. This block is set to perform a cyclic down sampling in multipath environment so that information can be gathered not only from shortest path, but also from other longer paths. For example, if symbol frame $\left\{A_0,0,\ldots B_0,0,\ldots C_0,0\ldots\right\}$ are transmitted, but received chips become $\left\{A_0^0,A_0^1,\ldots B_0^0,B_{0,}^1,\ldots C_0^0,C_0^1\ldots\right\}$ due to the multipath delay,

where the superscript 0,1 indicate different paths, the cyclic down sampling firstly samples $\left\{A_0^0, B_0^0, \ldots C_0^0\right\}$ from path 0, then samples $\left\{A_0^1, B_0^1, \ldots C_0^1\right\}$ from path 1, and then from the rest of paths.

- Despreading

The despreading operation is achieved by the correlation of orthogonal user code and the output of deinterleaver block. If we consider the orthogonal user code as a length P vector, and the output of deinterleaver block is still in the matrix form, then the despreading operation can be performed by multiplication of user code vector and the matrix from the deinterleave block.

In traditional orthogonal spreading/despreading, user data spread by a specific code can only be recovered from a vector that corresponds to this spreading code. However, in this proposed system, each chip is overlapped into nearby chips. Therefore, the same bit of user data can be recovered from different received vectors by using the same code, while other bits will not be decoded because of the orthogonality of the codes. This operation can be illustrated in Figure 14.

In Figure 14, $C_{A,1}C_{A,2}C_{A,3}C_{A,4}C_{A,5}C_{A,6}$ and $D_{A,1}D_{A,2}D_{A,3}D_{A,4}D_{A,5}D_{A,6}$ are two orthogonal codes that spread user data c and d, the vector $\{AAAAAA\}$ is one row in the deinterleaved matrix that contains information of c and d, and $\{\text{xxxxxx}\}$ represents other vectors that correspond to neither c nor d. When code $C_{A,1}C_{A,2}C_{A,3}C_{A,4}C_{A,5}C_{A,6}$ despread with the example matrix, only the vector $\{AAAAAA\}$ can be decoded as c, while other rows are decoded as 0 because of the

orthogonality between spreading and despreading codes. Similarly, when despreading with code $D_{A,1}D_{A,2}D_{A,3}D_{A,4}D_{A,5}D_{A,6}$, only vector {*AAAAAA*} is decoded as *d* while others are decoded as zero.

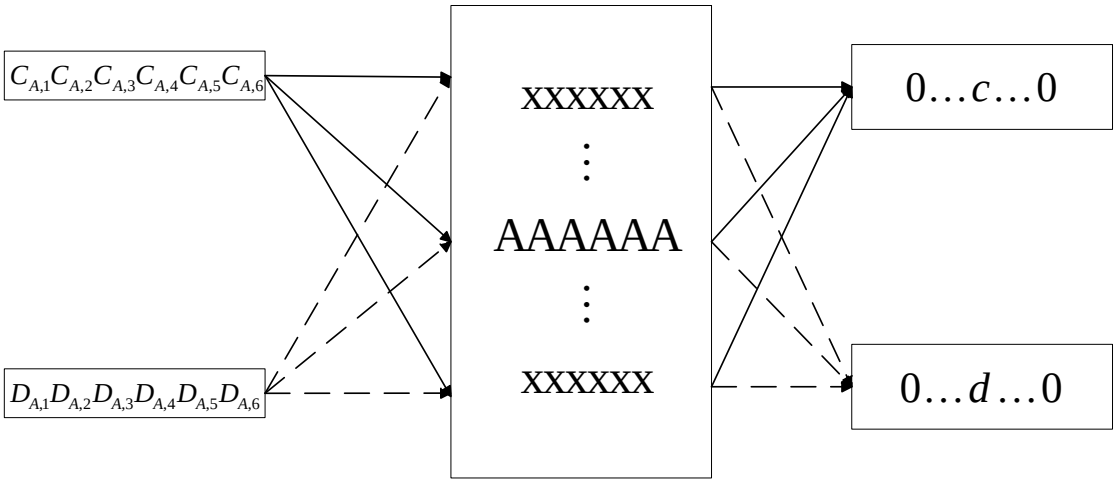

Figure 14. Example of despreading two bits (*c* and *d*) from the same bits (AAAAAA) using different code.

- Tap coefficient

The tap coefficient is used for channel equalization. Radio signal suffers significant fading and interference in a practical wireless channel, therefore channel equalizer is necessary in this system. Tap coefficients are estimated by training sequence.

3.5 Chapter Summary

System Models are introduced in this chapter. The DBDS system is formed by eight function blocks. Despite the simple structure, the transmitter end offers a high efficient function of spectrum reshaping without losing data rate, and the receiver end offers the ability of fully recovering signals from the bandwidth reshaped signals.

4 Algorithm

This chapter discusses the algorithm of dynamic bandwidth direct sequence. It will demonstrate mathematically how this proposed system can recover signals from partial bandwidth of the original MCIDS system while retaining the same data rate. This chapter is divided into two parts, one part is the algorithm in an ideal Gaussian channel, and the other part is the algorithm in multipath fading channel, which is closer to practical environment.

4.1 Algorithm in Ideal Gaussian Channel

In order to focus on investigating the possibility of recovering the signal through partial bandwidth, wireless channel is assumed to be a slow fading Gaussian channel. The received signal can be expressed as

$$r(t) = x(t) * h(t) + z(t) \tag{4.1}$$

where $x(t)$ is the transmitted signal, $h(t)$ is the filter and channel response, and $z(t)$ is the additive white Gaussian noise (AWGN) with double sided power spectral density $N_0/2$.

At the transmitter end, the traditional multicode interleaved sequence forms a block of user data $a_0, a_1, \ldots a_{N-1}$ with bit duration T_b , where, $a_i = \pm 1$ can be described mathematically as:

$$\sum_{i=0}^{N-1}\sum_{j=0}^{P-1} b_{\{i,j\}}\, g\left(t - iT_c - jNT_c\right) = \sum_{i=0}^{N-1} a_i \sum_{j=0}^{P-1} c_i \left[\left(j\right)_P\right] g\left(t - iT_c - jNT_c\right) \tag{4.2}$$

where $c_i\left[\left(j\right)_P\right]$ is the orthogonal spreading sequence with period P, $c_{i[(j)]} = \pm 1, j = 0,1,...P-1$ is one period of this periodic sequence with duration T_c and $\left[j\right]_P$ denotes j modulo P, $g(t)$ is defined as a unit amplitude pulse which is zero outside the interval $\left[0,T_c\right]$. In one period of multicode interleaving, N bits of user data are spread with P bits of orthogonal code for each bit of data. In ideal Gaussian channel, no multipath is involved, thus the CP is not required. Overall, there are $N \times P$ chips be produced during a period of multicode interleaving.

In ideal Gaussian channel, this sequence is directly shaped by a filter which adjusts chip bandwidth and spread information of each chip onto nearby chips. This filter can be set to half, quarter, one eighth or even less of the original sequence bandwidth, that is, after the filter, output sequence bandwidth is shaped into 2^{-m} of the original bandwidth, where $m = 1,2,3,\ldots$. At the receiver end, chips are also processed in $N \times P$ chip block together. The received signals are firstly sampled with sampling period T_c, then passed through a matched filter. Filters at transmitter and receiver ends together achieve the spectrum shaping purpose. Because those chips are still interleaved, and each chip has been overlapped into nearby 2^m chips, the filtered chip sequence in receiver end can be described as:

$$r\left(n\right) = \sum_{i=0}^{N-1} \sum_{j=-P_0}^{P-1} \alpha_{i,j} \sum_{k=i-2^m}^{i+2^m-1} a_k c_k \left[\left(j\right)_P\right] g\left[\left(n-i-jN\right)T_c\right] + z_n \qquad (4.3)$$

where $r(n)$ is the nth received sequence, z_n is the white discrete-time Gaussian noise, $\alpha_{i,j}$ are tap coefficients that related to the filter and channel response. Since the wireless channel is assumed to be slow fading channel, $\alpha_{i,j}$ can be treated as

constants. Note that $a_{-1}c_{-1}[(j)_P] = a_{k-1}c_{k-1}[(j)_P]$ because of the cyclic prefix in front of each signal block.

The despreading operation is the same as that in original MCIDS system [2] . Received chips are filled column-wisely into a $N \times P$ matrix. In order to perform despreading in the original MCIDS system, chips are simply read out in row-wise. However in this proposed system, chips are kept in the matrix for further processing. The remainder of $N \times P$ matrix is illustrated in Figure 15, denoting $E_{i,j} = \sum_{k=i-2^m}^{i+2^m-1} a_k c_k \left[(j)_P \right]$.

$$\begin{bmatrix} \alpha_{00}E_{00} + z_{00} & \alpha_{01}E_{01} + z_{01} & \cdots & \alpha_{0,P-1}E_{0,P-1} + z_{0,P-1} \\ \alpha_{10}E_{10} + z_{10} & \alpha_{11}E_{11} + z_{11} & \cdots & \alpha_{1,P-1}E_{1,P-1} + z_{1,P-1} \\ \alpha_{20}E_{20} + z_{20} & \alpha_{21}E_{21} + z_{21} & \cdots & \alpha_{2,P-1}E_{2,P-1} + z_{2,P-1} \\ \vdots & \vdots & \ddots & \vdots \\ \alpha_{N-1,0}E_{N-1,0} + z_{N-1,0} & \alpha_{N-1,0}E_{N-1,1} + z_{N-1,0} & \cdots & \alpha_{N-1,P-1}E_{N-1,P-1} + z_{N-1,P-1} \end{bmatrix}$$

Figure 15. Chips stored column wisely in $N \times P$ matrix.

Based on equation (3.1), each received chip contains information of nearby 2^m original chips. Therefore only $N / 2^m$ chips are required to recover all transmitted data. Thus, after down-sampling the above matrix in a row-wise manner by 2^m, the size of matrix now is $N/2 \times P$, and each sampled element in the matrix can be expressed as:

$$r(l+1, j+1) = \alpha_{2^m l, j} \sum_{k=2^m(l-1)}^{2^m(l+1)-1} a_k c_k \left[(j)_P \right] + z_{2^m l, j} \qquad (4.4)$$

where $l = 0,1,2,\ldots 2^{-m}N - 1$; $j = 0,1,2,\ldots P-1$. Down-sampled matrix $r_{l,j}$ with size $N/2^m \times P$ is shown in Figure 16

$$\begin{bmatrix} \alpha_{00}E_{00}+z_{00} & \alpha_{01}E_{01}+z_{01} & \cdots & \alpha_{0,P-1}E_{0,P-1}+z_{0,P-1} \\ \alpha_{2^m,0}E_{2^m,0}+z_{2^m,0} & \alpha_{2^m,1}E_{2^m,1}+z_{2^m,1} & \cdots & \alpha_{2^m,P-1}E_{2^m,P-1}+z_{2^m,P-1} \\ \alpha_{2^{m+1},0}E_{2^{m+1},0}+z_{2^{m+1},0} & \alpha_{2^{m+1},1}E_{2^{m+1},1}+z_{2^{m+1},1} & \cdots & \alpha_{2^{m+1},P-1}E_{2^{m+1},P-1}+z_{2^{m+1},P-1} \\ \vdots & \vdots & \ddots & \vdots \\ \alpha_{N-1-2^m,0}E_{N-1-2^m,0}+z_{N-1-2^m,0} & \alpha_{N-1-2^m,1}E_{N-1-2^m,1}+z_{N-1-2^m,1} & \cdots & \alpha_{N-1-2^m,P-1}E_{N-1-2^m,P-1}+z_{N-1-2^m,P-1} \end{bmatrix}$$

Figure 16. Rate 2^m down-sampled matrix.

For detection of each bit a_i in despreading, mathematically each row of the matrix is cyclically correlated with $P\times N$ bit long despread code $d_i[n]$. The despreading code is defined as

$$\begin{aligned} d_i[n] &= \sum_{j=0}^{P-1} c_i[j]\delta[n-i-jN] \\ i &= 0,1,\ldots N-1.\ n=0,1,\ldots PN-1 \end{aligned} \tag{4.5}$$

If we also put dispreading code into a $P\times N$ matrix, then the despreading operation can actually be performed as matrix multiplication of the $N/2^m \times P$ down-sampled receive-code matrix and the $P\times N$ despreading code matrix. Despread signals $U_{i,l}$ of code $d_i[n]$ at row l are overlapped components with contributions from nearby chips. Mathematically, we have

$$U_{i,l} = \sum_{j=0}^{P-1} r(l+1, j+1)\, c_i\left[(j)_P\right] \tag{4.6}$$

Suppose that U_i is the decision variable. This variable is obtained by the correlation of the despread signal $U_{i,l}$ and the conjugation of the corresponding tap coefficients $\alpha^*_{l,j}$. To collect energy from all l chips, we have

$$\begin{aligned} U_i &= \mathrm{Re}\left[\sum_{l=1}^{2^{-m}N} U_{i,l}\cdot\alpha^*_{2^m l,j}\right] \\ &= \mathrm{Re}\sum_{l=1}^{2^{-m}N}\sum_{j=0}^{P-1}\alpha^*_{2^m l,j}\alpha_{2^m l,j}\sum_{k=2^m(l-1)}^{2^{m(l+1)}-1} a_k c_k\left[(j)_P\right]c_P\left[(j)_P\right] + \mathrm{Re}\sum_{l-1}^{2^{-m}N}\alpha^*_{2^m l,j}\sum_{j=0}^{P-1} z_{2^m l,j} \end{aligned} \tag{4.7}$$

The calculation process of U_i using (4.6) and (4.7) is shown in **Error! Reference source not found.**.

Because $c_i\left[\left(j\right)_P\right]$ are orthogonal sequences, they satisfy

$$\sum_{k=2^m(l-1)}^{2^m(l+1)-1} a_k c_k\left[(j)_P\right] c_P\left[(j)_P\right] = \begin{cases} P, & i=k=l \\ 0, & otherwise \end{cases}. \tag{4.8}$$

When $i=k=l$, that is, when the spreading code matches the despreading code, the decision variable U_i becomes

$$U_i = P\sum_{l=1}^{2^{-m}N}\sum_{j=0}^{P-1}\left|\alpha_{2^m l,j}\right|^2 a_i + \mathrm{Re}\sum_{l=1}^{2^{-m}N}\sum_{j=0}^{P-1}\alpha^*_{2^m l,j} z_{2^m l,j}\,. \tag{4.9}$$

From the result we can tell, user data will be received only when the corresponding spreading code and despreading code are matched. In this situation, the final decision variable U_i will be an amplified value of original user data bit plus Gaussian noise. Otherwise, when spreading and despreading code are not matched, despread data will be zero with just Gaussian noise, and no other data bit that is spread or despread by other code is involved.

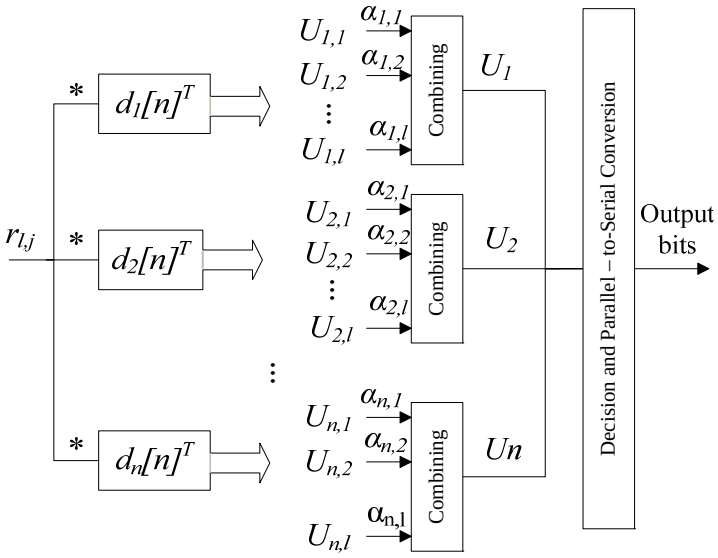

Figure 17. Dispreading and combining structure.

Hence, in ideal Gaussian channel, all user data can be fully recovered from 2^{-m} of original bandwidth by this method. The bit error can be expected to be only caused by Gaussian noise.

4.2 Algorithm in Multipath Fading Channel

In practice, multipath slow fading channel is much common in wireless transmission environment. This section will demonstrate how the purposed system recovers user data in multipath fading channel.

In multipath channel, signals through different paths arrive with different delays and thus cause the inter-symbol interference (ISI). The proposed system spread N bit user data with P bit code for each data, and processes $N \times P$ chips at a time. The output interleaved sequence can be recognized as P vectors with N chips in each vector. At the receiver end, P vectors are also processed together, and user data are

collected from every single vector. Due to the fact that transmitted chips are all interleaved, ISI between different received vectors can cause major distortion in output chips after deinterleaving and therefore significantly reduce system performance. ISI can also occur at chip level inside every received vector. The ISI from multipath fading channel will make filtered chips in every vector completely messed up. In that case, determination of channel estimation coefficients from received symbol will become extremely hard and easy to make mistake. Hence, the ISI in this system includes the ISI between chips in different vectors and the ISI between chips in the same vector. Both of them need a serious consideration.

As the solution to mitigate these two ISIs, three main changes at both transmitter end and receiver end are listed:

- Cyclic prefix is employed to suppress ISI between vectors.
- Symbol combiner is activated to compress every 2^m chip into one chip.
- The simple sampling operation at the receiver end is replaced by cyclic sampling.

To overcome the first ISI, this system employs cyclic prefix as ISI suppression between different received vectors. As long as multipath delays are no more than the duration of CP in each vector, ISI between vectors can be eliminated.

The method to solve the second ISI problem relies on the symbol combination operation at transmitter end. The combining operation row wisely merges element of every 2^m rows into one row, but retain the same matrix size. The elements in the first of every 2^m row are replaced by the respective sums of all 2^m rows, and the

remaining elements are set to zero. As Figure 13 shows, 2^m chips are combined into 1 chip, thus those 2^m chips will take the same amount of fading as well as filtering at the same time and will not become chaos during multipath transmission. Therefore, the tap coefficients that relate to filter and channel response for those 2^m original symbols will have the same value. This result means that detecting tap coefficient can be as easy as in ideal Gaussian channel. In other word, this will make the detection of tap coefficient much more accurate. Also because other original $2^m - 1$ chips are set to zero, a much larger gap between two reordered chips is produced, leads to a much higher tolerance of delay in the new sequence.

The combined sequence is in the form as

$$\{(a_0 + b_0 + c_0 + \ldots), 0, 0, \ldots, (a_1 + b_1 + c_1 + \ldots), 0, 0, \ldots, (a_2 + b_2 + c_2 + \ldots), 0, 0, \ldots, \}.$$

Assume the total multipath delays are less than 2^m chip duration. If we take $G_n = (a_n + b_n + c_n)$, and G_n^m is the received G_n from path m, then the received sequence will be $\{G_0^0, G_0^1, \ldots G_0^{m-1}, G_1^0 G_1^1, \ldots G_1^{m-1}, \ldots G_{n-1}^0 G_{n-1}^1, \ldots G_{n-1}^{m-1}\}$. The multipath delayed sequence is illustrated as Figure 18.

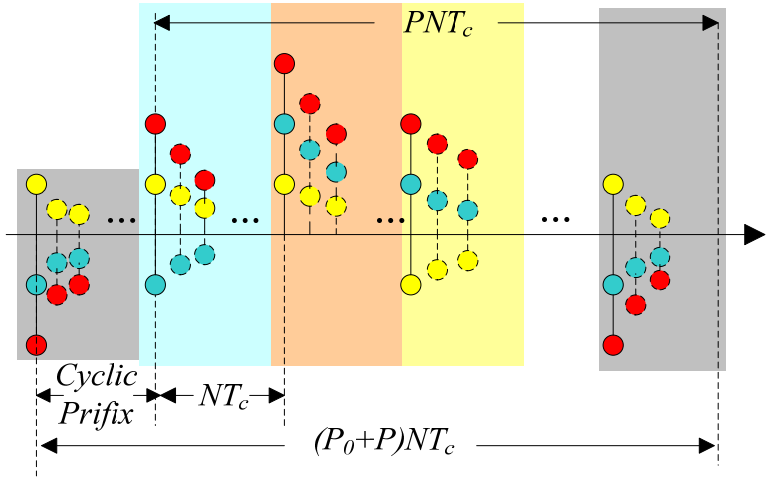

Figure 18. Combined sequence through multipath channel.

This combined sequence also brings a benefit that system performance can be improved by collecting all the energy of the chips from multiple paths. That is why simple sampling operation at the receiver end is replaced by cyclic sampling. For example, first we sample $\left\{G_0^0, G_0^1 \ldots G_0^{m-1}\right\}$, then $\left\{G_1^0, G_1^1 \ldots G_1^{m-1}\right\}$, all over to $\left\{G_{n-1}^0, G_{n-1}^1 \ldots G_{n-1}^{m-1}\right\}$. Each of those can be decoded using a decision variable of the same user data. By combining variables of multiple paths, miscoded variable can be corrected.

At the transmitter end, a multicode interleaved sequence with cyclic prefix can be expressed as (4.2). An easy way to achieve MCIDS with CP is to put spread symbols in row-wise into a matrix with $N+P$ rows and P rows, where the first P_0 row are CP, then output symbols in column-wise. The combination step after MCIDS can also be performed in this matrix, simply add every group of 2^m rows together to take place of original row, leaving the remaining rows zero. This process can be shown as Figure 19

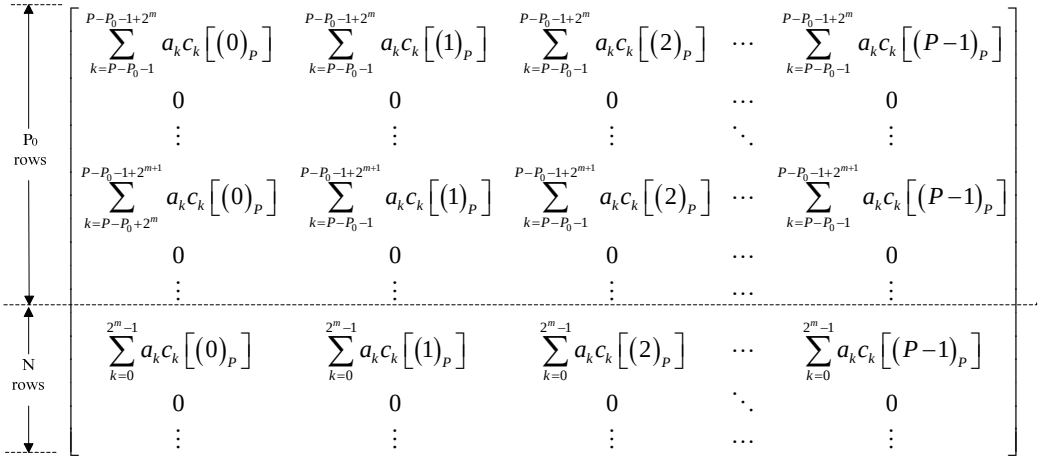

Figure 19. Row combination in matrix.

Interleaved sequence from the output of this matrix then is spectrum shaped by filter. Same as before, the filter type can be high pass, low pass, band pass, band block that limits output bandwidth to be 2^{-m} of original input, where $m = 0,1,2,\ldots$.

We assume the channel is multipath fading channel with Gaussian noise. Considering the multipath, we also assume no more than $2^m - 1$ total paths, the received signal can be generally expressed as (4.1). Interleaved chips here are also column-wisely filled into $(N + P_0) \times P$ matrix, where N is the N th data bit. Then, all the P_0 rows of CPs are removed to suppress ISI from different vector.

Take $G_{i,j} = \sum_{k=i\square 2^m-1}^{(i+1)2^m-1} a_k c_k \left[\left(j \right)_P \right]$ as the reordered chip, where $i = 0,1,\ldots (N-1)/2^m$, where $m = 0,1,2,\ldots$ and $E_{i,j} = \sum_{k=i-2^m}^{i+2^m-1} G_{k,j}$ indicates that 2^m of nearby chips are overlapped by filtering. After transmit through multipath channel, zeros in transmitted sequence will be overlapped by none zero chip G. Combined with filtering and multipath delay, the received matrix with CP removed can be illustrated as Figure 20.

$$\begin{bmatrix} \alpha_{00}E_{00}+z_{00} & \alpha_{01}E_{01}+z_{01} & \cdots & \alpha_{0,P-1}E_{0,P-1}+z_{0,P-1} \\ \alpha_{10}E_{00}+z_{10} & \alpha_{11}E_{01}+z_{11} & \cdots & \alpha_{1,P-1}E_{0,P-1}+z_{1,P-1} \\ \vdots & \vdots & \ddots & \vdots \\ \alpha_{2^m,0}E_{10}+z_{2^m,0} & \alpha_{2^m,1}E_{11}+z_{2^m,1} & \cdots & \alpha_{2^m,P-1}E_{1,P-1}+z_{2^m,P-1} \\ \alpha_{2^m+1,0}E_{10}+z_{2^m+1,0} & \alpha_{2^m+1,1}E_{11}+z_{2^m+1,1} & \cdots & \alpha_{2^m+1,P-1}E_{1,P-1}+z_{2^m+1,P-1} \\ \vdots & \vdots & \ddots & \vdots \\ \alpha_{2^m k,0}E_{k,0}+z_{2^m k,0} & \alpha_{2^m k,1}E_{k,1}+z_{2^m k,1} & \cdots & \alpha_{2^m k,P-1}E_{k,P-1}+z_{2^m k,P-1} \\ \alpha_{2^m k+1,0}E_{k,0}+z_{10} & \alpha_{2^m k+1,1}E_{k,1}+z_{11} & \cdots & \alpha_{2^m k+1,P-1}E_{k,P-1}+z_{2^m k+1,P-1} \\ \vdots & \vdots & \ddots & \vdots \end{bmatrix}$$

Figure 20. Multipath delayed sequence stored in matrix.

In Figure 20, z_n is the white discrete-time Gaussian noise, α are tap coefficients that are related to the filter and channel response. Since the wireless channel is assumed to be slow fading channel, $\alpha_{i,j}$ can be treated as constants. Note that $a_{-1}c_1 = a_{N-1}c_{N-1}$ due to the cyclic prefix in front of each signal block.

From Figure 20, it is clear that each received chip contains information of nearby 2^m original samples, and every 2^m chip in column contains the same user bits. Therefore only $N/2^m$ chips are required to recover all transmitted data. However collecting energy of all paths by cyclic sampling can improve system performance. Here we take out one row from every 2^m row for example. Based on Figure 20, the element in $k+1$ th row and $j+1$ th column in down sampled matrix can be express as

$$r(k+1, j+1) = \alpha_{2^m k,j}E_{k,j} + z_{2^m k,j} \tag{4.10}$$

where $l = 0,1,2,\ldots 2^{-m}N-1;\ j = 0,1,2,\ldots P-1$. As chips from different paths contain the same information as the original, the cyclic down sampled elements from different

paths are just repeats of the same information. Therefore, we can just use one group of the sampled matrix as a demonstration of the algorithm. The processing applies to the sampled matrix which collected from other paths. Down-sampled matrix $r_{l,j}$ with size $N/2^m \times P$ is shown in Figure 21.

$$\begin{bmatrix} \alpha_{00}E_{00}+z_{00} & \alpha_{01}E_{01}+z_{01} & \cdots & \alpha_{0,P-1}E_{0,P-1}+z_{0,P-1} \\ \alpha_{2^m,0}E_{10}+z_{2^m,0} & \alpha_{2^m,1}E_{11}+z_{2^m,1} & \cdots & \alpha_{2^m,P-1}E_{1,P-1}+z_{2^m,P-1} \\ \vdots & \vdots & \ddots & \vdots \\ \alpha_{2^m k,0}E_{k0}+z_{2^m k,0} & \alpha_{2^m k,1}E_{k1}+z_{2^m k,1} & \cdots & \alpha_{2^m k,P-1}E_{k,P-1}+z_{2^m k,P-1} \end{bmatrix}$$

Figure 21. Rate 2^m Down-sampled matrix.

The dispreading operation performs as a matrix multiplication for the down-sampled matrix and the dispreading vector. The *n*th dispreading code is still defined as

$$\begin{aligned} & d_i[n]=\sum_{j=0}^{P-1} c_i[j]\delta[n-i-jN] \\ & i=0,1,\ldots N-1, n=0,1,\ldots PN-1 \end{aligned} . \qquad (4.11)$$

In detection of each bit a_i, each row of the matrix is cyclically correlated with $d_i[n]$. Dispread signals $U_{i,l}$ of code $d_i[n]$ and row l, are overlapped components with contributions from nearby l chips. Mathematically, we have

$$U_{i,l}=\sum_{j=0}^{P-1} r(l+1, j+1)c_i[(j)_P]. \qquad (4.12)$$

Suppose that U_i is the decision variable. This variable is obtained by correlation of dispread signal $U_{i,l}$ and conjugate of corresponding tap coefficients $\alpha_{l,j}^*$. To collect energy from all l chips, we have

$$
\begin{aligned}
U_i &= \mathrm{Re}\left[\sum_{l=1}^{2^{-m}N} U_{i,l}\cdot\alpha^*_{2^m l,j}\right] \\
&= \mathrm{Re}\left[\sum_{l=1}^{2^{-m}N}\sum_{j=0}^{P-1}\left(\alpha_{2^m l,j}E_{i,j}+z_{2^m l,j}\right)\cdot\alpha^*_{2^m l,j}\right] \\
&= \mathrm{Re}\sum_{l=1}^{2^{-m}N}\sum_{j=0}^{P-1}\alpha^*_{2^m l,j}\alpha_{2^m l,j}\sum_{i=n-2^m}^{n+2^m-1}\sum_{k=2^m l-1}^{2^m(l+1)-1}a_k c_k\left[(j)_P\right]c_i\left[(j)_P\right]+\mathrm{Re}\sum_{l=1}^{2^{-m}N}\sum_{j=0}^{P-1}\alpha^*_{2^m l,j}z_{2^m l,j}
\end{aligned}
\quad . \qquad (4.13)
$$

Because $c_i\left[(j)_P\right]$ are orthogonal sequences, they satisfy

$$
\sum_{i=n-2^m}^{n+2^m-1}\sum_{k=2^m(l-1)}^{2^m(l+1)-1}c_k\left[(j)_P\right]c_i\left[(j)_p\right]=\begin{cases}P, & i=k=l=n\\ 0, & otherwise\end{cases}. \qquad (4.14)
$$

When $i=k=l=n$, that is, when the correspond spreading code and dispreading code match, the decision variable U_i becomes

$$
U_i = P\sum_{l=1}^{2^{-m}N}\sum_{j=0}^{P-1}\left|\alpha_{2^m l,j}\right|^2 a_i+\mathrm{Re}\sum_{l=1}^{2^{-m}N}\sum_{j=0}^{P-1}\alpha^*_{2^m i,j}z_{2^m i,j}\,. \qquad (4.15)
$$

In multipath channel, we can see that even though the ISI effect causes serious disorder in the received chips, user data can still be drawn when the corresponded spreading code and dispreading code match each other.

4.3 Chapter Summary

Based on the above mathematical analysis, it is proved that through multicode interleaving, filtering, symbol combining, cyclic down sampling, the DBDS system can fully recover user data under variety of limited bandwidths due to the orthogonality of spreading/dispreading code. However, the limited bandwidth must be in the form of half bandwidth, quarter bandwidth, 1/8 bandwidth, etc.

5 Simulation Structure

The simulation platform is built on Simulink 2006a by the Mathworks. All function blocks in the simulation are either build-in Simulink blocks or user-defined blocks. Based on system model in Figure 10, the coming sections of this chapter will demonstrate the structure and implementation of Simulink model for dynamic bandwidth direct sequence system.

5.1 Simulation Structure of Transmitter

In Figure 10, the process of data stream for the transmitter is described as follows: the data stream is modulated into BPSK, and then spread by an orthogonal code. Each data bit is spread into a frame, and multiple frames are interleaved under MCIDS algorithm and form one big frame. In ideal channel assumption, the interleaved frames are directly filtered by a spectrum shaping filter. In multipath Gaussian channel, several chips are merged into one chip and leave other chips zero before the filtering. Figure 22 shows the structure of the subsystem of DBDS transmitter.

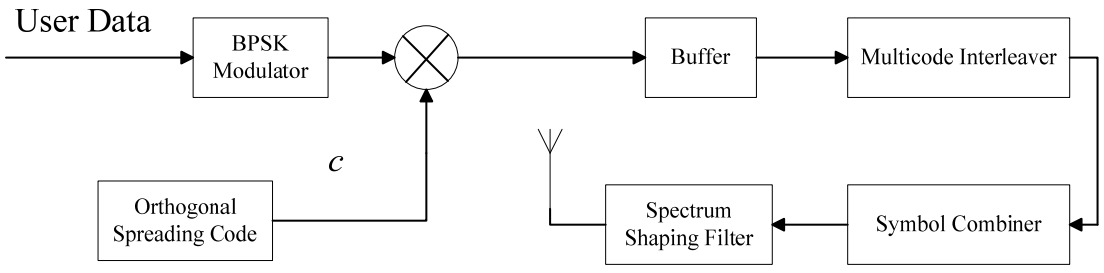

Figure 22. The DBDS transmitter structure.

Functions of blocks and settings are:

- BPSK modulator

In simulation, user data are produced by a random binary generator. In order to simplify the system, user data are set to be frame based real BPSK.

- Spreading

Multiplication of user data and orthogonal spreading code accomplishes spreading operation. The orthogonality of code set may affect system performance. In our simulation, the Hadamard code is chosen as this code set has a high orthogonality.

- Buffer

Multicode interleaving requires several chip frames in every processing loop, but encoded chips that continually come in are sample based. The buffer block is a bridge between spreader and multicode interleaver. It periodically gathers data sequences from spreader and buffers them into one frame so that the following multicode interleaver can be processed. Buffer size depends on the length of spreading code. If spreading code length is P, then buffer size is P^2.

- Multicode interleaver

This block performs the multicode interleaving operation and inserts a cyclic prefix (CP) for each P chips every time after a frame of buffered data is fed in. This block fills P^2 bit of chips into a $P \times P$ matrix in row wise. To insert CP, simply add the last P_0 rows above to the first row. Finally, this matrix is transferred into symbol combiner block.

- Symbol combiner

The combiner row wisely merges element of every 2^m rows into one row, but remains the same matrix size. Elements in the first of every those 2^m rows are replaced by the sums of all 2^m rows, and the remaining elements are set to zero. Finally, elements in matrix are output in column wise. The output chips are put in one frame for the convenience of later filtering. Note that this block does not need to be activated in ideal Gaussian channel environment. An inactivated combiner block does not merge any row in the matrix, just simply output the elements in column wise.

- Bandwidth adjusting filter

This block shapes the spectrum of chips and adjusts its bandwidth by using a certain digital filter. Based on the wireless channel environment and cognition requirement, filter employed in this block can be chosen from various high pass, low pass, band pass or band block filters. The adjusted bandwidth however must limit to 2^{-m} of original, such as $\frac{1}{2}, \frac{1}{4}, \frac{1}{8}$ of original bandwidth or etc. Before forwarding to the UWB channel, the frame-based chip is converted into sample based.

5.2 Simulation Structure of UWB Channel

UWB channel in our simulation is formed by two blocks, a multipath delay block plus an AWGN block. In the multipath block, a vector that represents fading component for each path is randomly generated based on the path number and normalized power. Each path causes an additional delay of 1 chip duration.

Values in path vector are generated in the following way. Despite the different number of paths, total energy of all paths is 1. Those values are randomly generated in average of one over the path number, with a certain amount of mean square error. For example, this vector can be in the form like $\{0.4 \quad 0.3 \quad 0.2 \quad 0.1\}$, which means in total 4 paths, 40% of energy comes from line of sight, 30% of energy has 1 chip delay, 20% has 2 chips delay, and 10% has 3 chips delay. The path number is set to be the minimum between bandwidth adjusting number 2^m and length of prefix P_0. Transmitted symbols are convolved with this vector to simulate the effect of multipath.

5.3 Simulation Structure of Receiver

Figure 23 lists the structure of receiver also based on Figure 10. At receiver end, received chips are firstly passed through a matched filter, and then deinterleaved in a $(P+P_0)\times P$ matrix. Next, matrix is row-wisely down sampled after removal of its cyclic prefix. By despreading cyclic sampled matrix with orthogonal code, the corresponding variable can be detected.

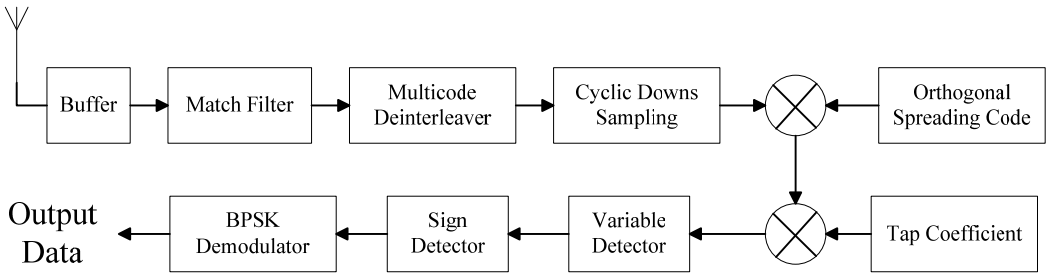

Figure 23. The DBDS receiver structure.

Functions of each block at the receiver end are:

- Buffer

This buffer collects sampled chips from antenna and converts sampled chips into a $(P+P_0)\times P$ bit long frame.

- Match filter

Match filter at receiver end co-works with bandwidth adjusting filter at the transmitter end. Together they complete the spectrum shaping for the chip sequence. This filter uses the same settings and parameters of the filter in transmitter end.

- Multicode deinterleaver

In receiver end, the multicode deinterleaver operates exactly in reverse order of the interleaver. Interleaved chips at here are also column-wisely filled into $(P+P_0)\times P$ matrix. Then, all the P_0 rows of CP are removed to suppress ISI between different vectors. Matrix size now becomes $P\times P$.

- Cyclic down sampling

In this step, chips in matrix are down sampled at rate 2^m. At receiver end, information is overlapped from one chip into nearby 2^m chips as explained before. Therefore, only one in every 2^m chips is required. In multipath channel, signals from different path may overlap onto the next couple of chips. Therefore in this situation, corresponding data can also be collected from the next couple of chips. This block is set to perform a cyclic down sampling in multipath environment so that it can not only gather information from shortest path but also from other longer paths. Note that

in ideal Gaussian channel, cyclic sampling is not necessary, only regular down sampling at rate 2^m is needed.

- Despreading

Despreading operation is achieved by the correlation of orthogonal user code and the output of deinterleaver block. In the simulation, both the spreading code and despreading code are the same code generated by the same function block. In our programme, because chips are stored in matrix, the despreading operation can be easily achieved by matrix multiplication of the sampled $2^{-m}P \times P$ matrix and the P length vector of orthogonal code. Output of this block is the $U_{i,l}$ in (4.6), which is also a P length vector.

- Tap coefficient

The $P \times P$ matrix stores the entire channel coefficient $\alpha_{l,j}$ that needed. This matrix is calculated by a training sequence that both transmitter and receiver know. Before sending user data, a P bit long training sequence is transmitted. This sequence is processed in the same regular way in the system, such as encoding, multicode interleaving, symbol combing, filtering at transmitter end, and match filtering, multicode deinterleaving, down sampling, despreading at receiver end. Initially, tap coefficient is set to be a $P \times P$ unit matrix. At transmitter end, spread user data are buffered into a $P \times P$ matrix, we mark it as matrix A. Next, after the despreading, we will have another $P \times P$ matrix marked as B. As matrix B at receiver end is the un-equalized version of matrix A, we can find out the coefficient matrix by comparing every element between matrix A and B.

- Variable detection

Decision variable U_i comes from the multiplication of despread result $U_{i,l}$ and its related tap coefficient. Every row in tap coefficient is set for a specific $U_{i,l}$. For example, the first row of the tap coefficient matrix correlates with the very first $U_{i,l}$ frame, which corresponds to the first user data bit, and to detect the second U_i, the second row in tap coefficient matrix is multiplied by the second $U_{i,l}$ frame.

- Sign detector

This block judges the sign of decision variable U_i. If U_i is positive, then output $\{+1\}$, or if negative, then output $\{-1\}$.

- BPSK demodulator

This block converts $\{+1\}$ and $\{-1\}$ into binary user data.

5.4 Chapter Summary

This chapter describes the function and block design in our simulation program. The Simulink models that used in the simulation are built based on the instruction of system model that mentioned in Chapter 4. Note that in simulation, certain delays for the dispreading code must be considered to guarantee the correct timing for spreading/dispreading. Also some necessary buffers are used in between some blocks for the processing convenience.

6 Result Analysis and Discussion

This chapter covers simulation results and analysis based on the results. Furthermore, future work over dynamic bandwidth direct sequence UWB system is also discussed. Table 1 lists all the parameters used in the simulation.

Table 1. General setting

Name	Parameter	Note
User data period	4×10^{-8} seconds	User data rate is 25M bps
Orthogonal code length	16 bit	Transmit bandwidth is spread to 400M bps
Modulator type	Real BPSK	
Run Time	100,000	
Cyclic prefix length	4 bit	Expecting to cause 2-3 dB BER-Eb/No loss

Simulations under ideal Gaussian channel and multipath channel are performed. In each simulation, bandwidth adjustments of 1/2 and 1/4 are tested.

6.1 Simulation in Ideal Gaussian Channel

Simulation parameter in idea Gaussian channel is listed in Table 2.

Table 2. Settings for idea Gaussian channel

Name	Parameter	Note
Bandwidth adjusting rate	Normalized 1/2 or 1/4 bandwidth	Limit data bandwidth into half or quarter of original
Filter type	Raised Cosine filter(low pass), High pass, Band pass	Low pass filter limits output band to the lower half or quarter part in spectrum; High pass filter limits band to the higher half in spectrum, and band pass filter limits transmitted band to the central half in spectrum.

The BER-Eb/No results of ideal Gausian channel is shown in Figure 24. From the results we can see that limiting transmission bandwidth into a half or a quarter of the original bandwidth does not harm bit error rate of the DBDS system, which means that data rate will not change. Also we can see that in ideal Gaussian channel, the BER-Eb/No curve of this system matches the theoretical result. It provides strong evidence that DBDS system is a lossless transmission algorithm.

Now let us see the BER-Eb/No result with 4 bit CP, which shown in Figure 24 and Figure 26. From these two results, it is clear that system performance will not be affected by the type of filters. Therefore user can choose any suitable filters to satisfy the cognitive needs. A 4 bit CP is employed to suppress ISI, however due to the processing gain loss, the system is expected to have 2 to 3 dB loss which is proven by the BER-Eb/No curves in Figure 25 and Figure 26 .

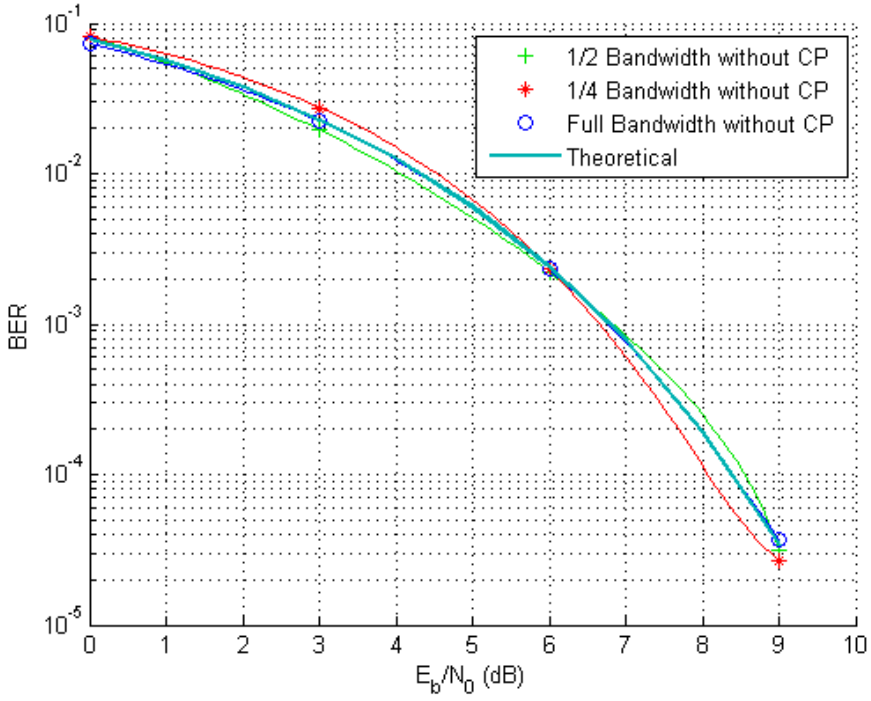

Figure 24. Average performance for raised cosine filter under ideal Gaussian channel without CP.

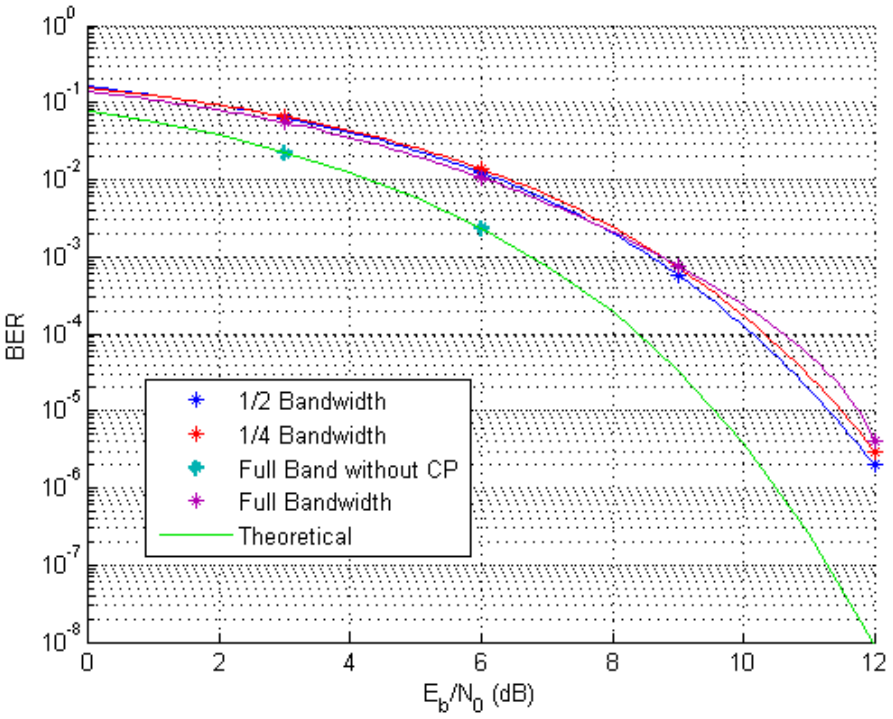

Figure 25. Average performance using raised cosine filter with 4 bit CP in ideal Gaussian channel.

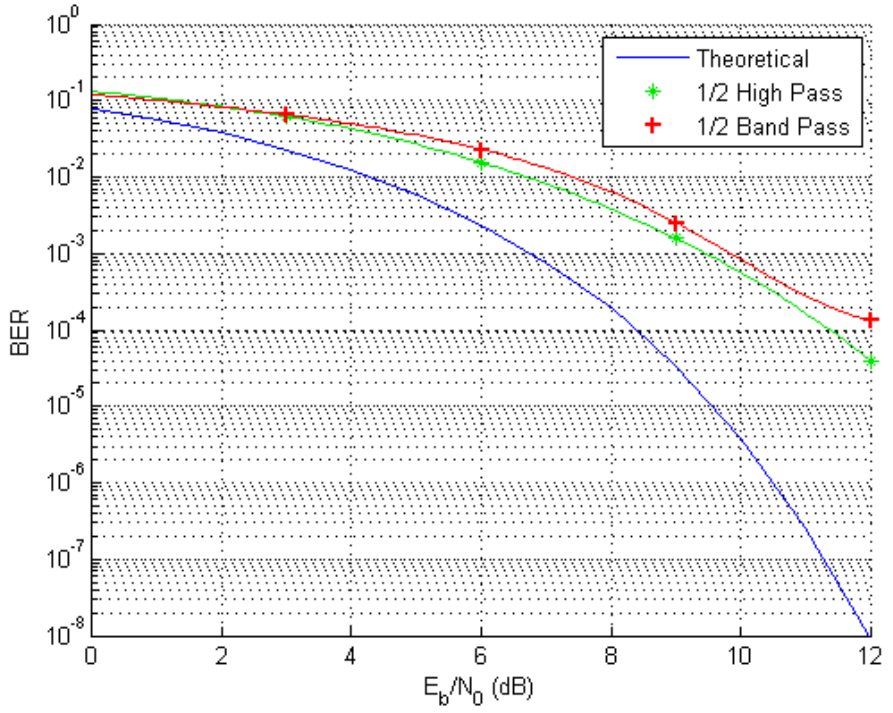

Figure 26. Average performance using half bandwidth high pass and low pass filter with 4 bit CP in ideal Gaussian channel.

6.2 Simulation in Multipath Gaussian Channel

Figure 27 shows system performance that transmission band is limited by half bandwidth band pass filter and high pass filter. This figure shows again that performance will not be affected by different type of filter. Also comparing this figure with average BER-Eb/No curve in ideal Gaussian channel, no significant performance lost can be found. The loss is only about 0 to 1 dB.

The Simulation parameters in multipath Gaussian channel are listed in Table 3.

Table 3. Settings for multipath Gaussian channel

Name	Parameter	Note
Bandwidth adjusting rate	Normalized 1/2 or 1/4 bandwidth	Limit data bandwidth into half or quarter of original
Filter type	Raised cosine filter (low pass), High pass, Band pass	Low pass filter limits output band to the lower half or quarter part in spectrum; High pass filter limits band to the higher half in spectrum, and band pass filter limits transmitted band to the central half in spectrum.
Multipath number	2 in 1/2 filter and 4 in 1/4 filter	Note
Bandwidth adjusting rate	Normalized 1/2 or 1/4 bandwidth	Limit data bandwidth into half or quarter of original

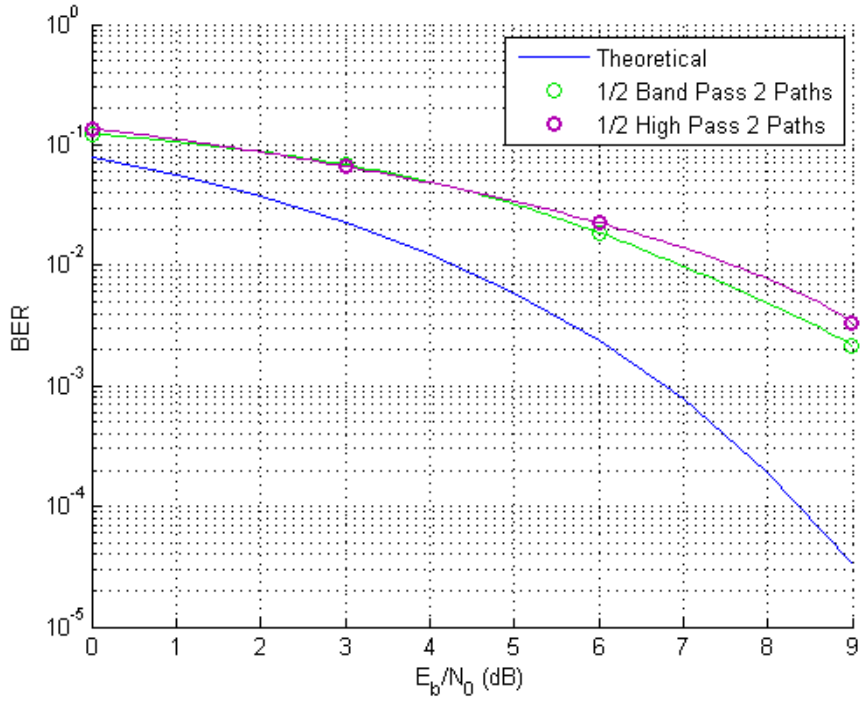

Figure 27. Average performance by half bandwidth (a) band pass and (b) high pass filter under multipath Gaussian channel.

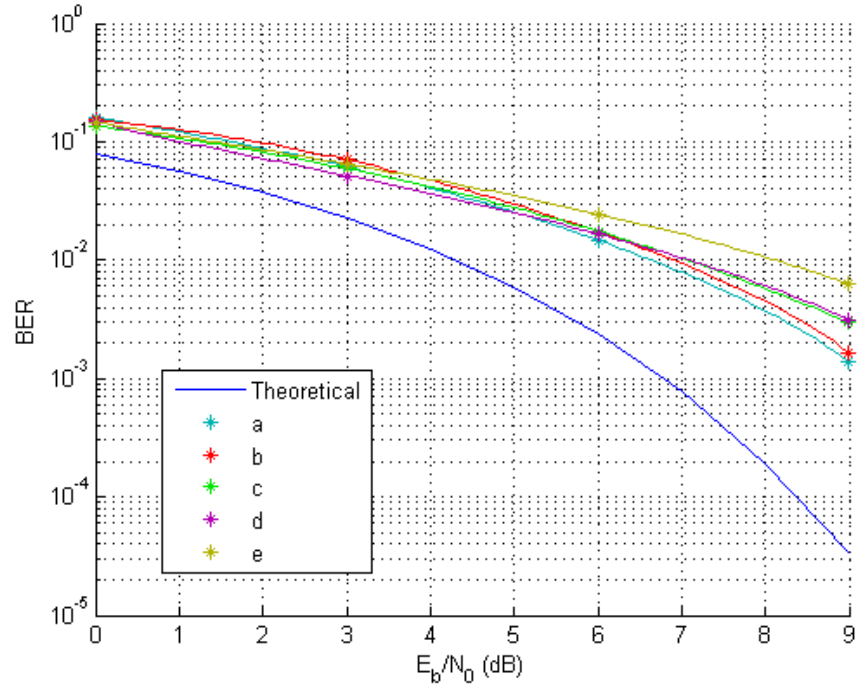

Figure 28. Average performance with (a). 1/2 band low pass filter in 2 paths channel; (b). 1/4 band low pass filter in 4 path channel; (c). 1/4 high pass filter in 3 path channel; (d). 1/4 high pass filter in 4 path channel; (e).1/4 band pass filter in 4 path channel.

Figure 28 shows more average BER-Eb/No curves of the system performance under different type of filter and different bandwidths.

From Figure 28 we can confirm again that system performance remains stable under different transmission bandwidths and different shapes of spectrum, even in multipath channel, as long as the multipath delay is less than the minimal value of CP duration and 2^m chip duration, if transmission bandwidth is limited to 2^{-m} of the original bandwidth.

6.3 Discussion

In ideal Gaussian channel, the DBDS system offers a lossless solution for cognitive UWB. Its BER curves match the theatrical curve, even though transmission bandwidth has already been limited into half or quarter of original. The only performance loss is caused by cyclic prefix.

In multipath Gaussian channel, the DBDS system combines every 2^m of chips into one in between interleaving and filtering step. By doing this operation, interleaved 2^m symbols are forced to face same level of variation when transmitted in multipath fading channel. Performance loss caused by the difficulty in detecting tap coefficients for each symbol is overcome. DBDS system under multipath channel provides performance close to that in ideal Gaussian channel, which is very impressive.

Compared to traditional direct sequence based UWB transmission, the DBDS system can fully recover user data from different transmission bandwidth. Furthermore, according to all the simulation results under different channels, different transmission bandwidths, and different spectrum shaping filters, the DBDS system offers the same bit error rate as the full bandwidth transmission. This result gives the evidence that the DBDS system can transmit in limited bandwidth while retaining the same speed of data rate.

Due to this advantage provided by the new dynamic bandwidth direct sequence system, direct sequence based UWB system now can have a much easier and efficient way to achieve cognition. This system enables multiple wireless UWB devices to share the same spectrum. For example, one uses lower half of the available spectrum, and another uses upper half of it, but none of them will have data rate lost or interference between them.

Future work on this research will focus on implementation in hardware. Also, a protocol over DBDS system needs to be designed. This protocol deals with coexistence issue between multiple DBDS systems as well as interference issue between DBDS system and narrow band systems. It should have the ability to define the amount of bandwidth adjustment and the shape of adjusted bandwidth based on real time environment.

6.4 Chapter Summary

This chapter presents the simulation results based on the proposed DBDS system. Firstly, simulations in ideal Gaussian channel are examined by different filters, including high pass, low pass and band pass filters. Reshaped bandwidth is reduced into a half and a quarter of the original bandwidth. Later, this system is also tested in multipath channel with the same filters. In both scenarios the DBDS system provides a very good performance.

7 Conclusions

The new dynamic bandwidth direct sequence (DBDS) UWB system is proposed in this thesis as a novel cognitive solution for DS based UWB. UWB technology occupies a large range of bandwidth. Transmission of UWB signals in full bandwidth will unavoidably interfere with narrow band transmission or other UWB transmission in the same area. This fact makes UWB technology even more dependent on cognitive radio. Current cognitive radio solutions for DS based UWB are mainly focused on pulse generation, trying to produce a specific impulse according to working spectrum environment. Large amount of calculation involved in those methods seriously increases system complexity. Meanwhile, generated impulse normally has much longer duration, which unavoidably limits date rate. Under this situation, any approach of cognitive UWB without decreasing transmission date rate and significant change of system complexity would all be considered remarkable.

DBDS is a new DS based UWB system, featuring wireless communication under much lower transmission bandwidth but retaining the same transmission rate. With multi-code interleaving, symbol combining, bandwidth filtering and cyclic down sampling, this system is able to dynamically compress its transmission into half, quarter, one eighth or even less of the original bandwidth without deceasing its data rate. This system can fully recover signals at different transmission bandwidth and different transmission band, only slightly increases system complexity comparing to the full bandwidth system. When most of other cognitive UWB approaches focus on generating specific UWB impulse under the FCC spectrum mask, DBDS alternatively achieves bandwidth adjustment in another way. It does not require specific impulse generation. It dynamically adjusts transmission bandwidth in lossless data rate and

still keeps a very simple structure. Thus, the DBDS system provides another efficient cognitive solution for DS based UWB.

This system is proven to have a very impressive cognitive performance by the software simulation. Future work will concentrate on implementation in hardware platform and protocol design to allow multiple DBDS devices work in practice.

8 References

[1] M. Bettayeb and S. F. A. Shah, "State of the art ultra-wideband technology for communication systems: a review," Proc. 10th IEEE International Conference on Electronics, Circuits and Systems, 2003.

[2] X. Huang and Y. Li, "The multicode interleaved DSSS system for high speed wireless digital communications," Proc. ICC 2001.

[3] J. Lorincz and D. Begusic, "Physical layer analysis of emerging IEEE 802.11n WLAN standard," Proc. The 8th International Conferenceon Advanced Communication Technology, 2006.

[4] R. Fontanna, "A brief history of UWB communications," 2004.

[5] Bennett, C. Leonard, and G. F. Ross, "Time – domain electronmagetics and its applications," Proc. IEEE 66, 1978.

[6] Intel, "Ultra-wideband (UWB) technology," 2008, Available at http://www.intel.com/technology/comms/uwb/.

[7] V. Cossiavelou, "An examination of select wireless technologies in the Asia-Pacific market," Proc. Wireless Telecommunications Symposium, 2006.

[8] H. Wen and Z. Guoxin, "Orthogonal Hermite pulses used for UWB M-ary communication," Proc. International Conference on Information Technology: Coding and Computing, 2005.

[9] X. Huang and Y. Li, "The spectral evaluation and comparison for ultra-wideband signals with different modulation schemes," Proc. World Multiconference on Systemics, Cybernetics and Informatics, Orlando, Florida, USA, 2000.

[10] X. Huang and Y. Li, "Generating near-white ultra-wideband signals with period extended PN sequences," Proc. 53rd Vehicular Technology Conference, IEEE, 2001.

[11] O. S. Shin, S. S. Ghazzemzadeh, L. J. Greenstein, and V. Tarokh, "Performance evaluation of MB-OFDM and DS-UWB systems for wireless personal area networks," Proc. IEEE International Conference on Ultra-Wideband, 2005.

[12] D. Sorte, M. Femminella, G. Reali, and S. Zeisberg, "Network service provisioning in UWB open mobile access networks," *IEEE Journal on Selected Areas in Communications*, vol. 20, pp. 1745-1753, 2002.

[13] G. Bellusci, Y. Junlin, G. J. M. Janssen, and C. C. J. Tiberius, "An ultra-wideband positioning demonstrator using audio signals," Proc. 4th Workshop on Positioning, Navigation and Communication, 2007.

[14] A. Batra, J. Balakrishnan, and A. Dabak, "Multi-band OFDM: a new approach for UWB," Proc. International Symposium on Circuits and Systems, 2004.

[15] R. Kolic, "Ultra wideband - the next-generation wireless connection," 2004, Available at http://www.intel.com/technology/magazine/communications/wi02042.pdf.

[16] Y. Ishiyama and T. Ohtsuki, "Performance evaluation of UWB-IR and DS-UWB with MMSE-frequency domain equalization (FDE)," Proc. Global Telecommunications Conference, IEEE, 2004.

[17] F. Nekoogar, "Applications and target markets," in *Ultra-Wideband Communications Fundamentals and Applications*. Sydney: Prentice Hall PTR, 2006, pp. 151-174.

[18] C. Lee and J. Y. Kim, "UWB communication and networking systems with chaotic oscillator for low rate WPAN," Proc. The 8th International Conference of Advanced Communication Technology, 2006.

[19] L. Xue Jun, C. Peter Han Joo, C. Kok Shyang, Yee Hui Lee, and Ping Shum, "Design and implementation of a UWB peer-to-peer communication network," Proc. 6th International Conference on Information, Communications & Signal Processing, 2007.

[20] M. P. Wylie-Green, P. A. Ranta, and J. Salokannel, "Multi-band OFDM UWB solution for IEEE 802.15.3a WPANs," Proc. IEEE/Sarnoff Symposium on Advances in Wired and Wireless Communication, 2005.

[21] R. S. Vickers, "Design and applications of airborne radars in the VHF/UHF band," *Aerospace and Electronic Systems Magazine, IEEE*, vol. 17, pp. 26-29, 2002.

[22] K. M. Strohm, H. L. Bloecher, R. Schneider, and J. Wenger, "Development of future short range radar technology," Proc. European Radar Conference, 2005.

[23] J. Wenger, "Automotive radar - status and perspectives," Proc. Compound Semiconductor Integrated Circuit Symposium, IEEE, 2005.

[24] G. Desoli and E. Filippi, "An outlook on the evolution of mobile terminals: from monolithic to modular multiradio, multiapplication platforms," *Circuits and Systems Magazine, IEEE*, vol. 6, pp. 17-29, 2006.

[25] V. Rodriguez and F. Jondral, "Market-driven regulation for next generation ultra-wide-band technology: Technical-economic management of a 3G cell with coexisting UWB devices," Proc. Mobile and Wireless Communications Summit, 2007.

[26] B. Krenik, "Cellular handset evolution - convergence of high-speed data services," Proc. Radio Frequency Integrated Circuits (RFIC) Symposium, IEEE, 2004.

[27] D. E. Anagnostou, S. Nikolaou, K. Hyungrak, K. Boyon, M. Tentzeris, and J. Papapolymerou, "Dual band-notched ultra-wideband antenna for 802.11a WLAN Environments," Proc. Antennas and Propagation International Symposium, IEEE, 2007.

[28] J. McCorkle, "Ultra wide bandwidth (UWB): gigabit wireless communications for battery operated consumer applications," Proc. VLSI Circuits, Digest of Technical Papers, 2005.

[29] B. Q. Ruiz, A. A. Vazquez, M. L. Rubio, and J. L. G. Garcia, "Impulse radio UWB system architecture for smart wireless sensor networks," Proc. 2nd International Workshop in Networking with Ultra Wide Band and Workshop on Ultra Wide Band for Sensor Networks, , 2005.

[30] NTIA, "U.S. frequency allocations," Available at: http://www.ntia.doc.gov/osmhome/allochrt.pdf.

[31] X. Chu and R. D. Murch, "The effect of NBI on UWB time-hopping systems," *Wireless Communications, IEEE Transactions*, vol. 3, pp. 1431-1436, 2004.

[32] S. S. Choi and W. J. Oh, "Analysis the interference of pulse position modulated UWB into IEEE 802.11 a WLAN," Proc. International Workshop on Ultra Wideband Systems, Joint with Conference on Ultrawideband Systems and Technologies, 2004.

[33] F. Granelli and H. Zhang, "Cognitive ultra wide band radio: a research vision and its open challenges," Proc. 2nd International Workshop Networking with

Ultra Wide Band and Workshop on Ultra Wide Band for Sensor Networks, 2005.

[34] "Spectrum Policy task force report," Federal Communications Commission Tech. Rep. TR 02-155, 2002.

[35] D. Cassioli, R. Giuliano, and F. Mazzenga, "Analysis of UWB system capacity in a realistic multipath environment with coexistence constraints," *Communications, IET*, vol. 1, pp. 391-397, 2007.

[36] J. Mitola, III, "Cognitive radio for flexible mobile multimedia communications," Proc. International Workshop on Mobile Multimedia Communications, IEEE, 1999.

[37] FCC, "Notice of proposed rule making and order," ET Docket No. 03-222, 2003.

[38] R. Mokhtar, S. Khatun, B. M. Ali, and R. Saeed, "Cognitive radio technology for flexible spectrum sharing," Proc. 4th Student Conference on Research and Development, 2006.

[39] M. E. Sahin, S. Ahmed, and H. Arslan, "The roles of ultra wideband in cognitive networks," Proc. International Conference on Ultra-Wideband. IEEE, 2007.

[40] D. Cabric, I. D. O'Donnell, M. S. W. Chen, and R. W. Brodersen, "Spectrum sharing radios," *Circuits and Systems Magazine, IEEE*, vol. 6, pp. 30-45, 2006.

[41] M. E. Sahin and H. Arslan, "A narrowband interference identification approach for UWB systems," Proc. Military Communications Conference, IEEE, 2005.

[42] Y. Zhao and S. G. Haggman, "Intercarrier interference self-cancellation scheme for OFDM mobile communication systems," *Communications, IEEE Transactions*, vol. 49, pp. 1185-1191, 2001.

[43] A. Batra, S. Lingam, and J. Balakrishnan, "Multi-band OFDM: a cognitive radio for UWB," Proc. International Symposium on Circuits and Systems, 2006.

[44] H. Yamaguchi, "Active interference cancellation technique for MB-OFDM cognitive radio," Proc. 34th European Microwave Conference, 2004.

[45] T. Dissanayake and K. P. Esselle, "Design of slot loaded band-notched UWB antennas," Proc. Antennas and Propagation Society International Symposium, IEEE, 2005.

[46] M. Lai and S. K. Jeng, "A microstrip three-port and four-channel multiplexer for WLAN and UWB coexistence" *IEEE Transactions on Microwave Theory and Techniques*, vol. 53, pp. 3244-3250, 2005.

[47] X. Zhou, K. Y. Yazdandoost, H. Zhang, and I. Chlamtac, "Cognospectrum: spectrum adaptation and evolution in cognitive ultra-wideband radio," Proc. IEEE International Conference on Ultra-Wideband, 2005.

[48] L. Wei, Z. Weixia, X. Fangmin, Z. Zhou, and K. S. Wei, "A novel frequency-band coded orthogonal UWB chirp pulse design for cognitive NBI suppression," Proc. International Symposium on Microwave, Antenna, Propagation and EMC Technologies for Wireless Communications, 2007.

[49] W. Zhang, H. Shen, and K. S. Kwak, "Pulse series based UWB CR system," Proc. International Workshop on Cross Layer Design, 2007.

[50] X. Zhou, H. Zhang, and I. Chlamtac, "Space-frequency coded cooperative scheme among distributed nodes in cognitive UWB radio," Proc. IEEE 16th

International Symposium on Personal, Indoor and Mobile Radio Communications, 2005.

[51] L. Huang, H. X. Zhang, and Y. H. Lu, "A novel method to generate UWB shaping pulses based on chip pulse," Proc. 6th International Conference on ITS Telecommunications Proceedings, 2006.

[52] P. He, Y. Lu, H. Zhang, and J. Lu, "A pulse shaping method for UWB avoiding the frequency coexistence interference with WLAN," Proc. 2nd International Conference on Mobile Technology, Applications and Systems, 2005.

[53] F. Xu, W. Zhong, and Z. Zhou, "Cognitive Interference suppress in UWB system using modified Hermite Polynomials pulse," Proc. Communications and Information Technologies, 2006.

[54] X. Huang, D. Lowe, R. Gandia, and E. Dutkiewicz, "An impulse ultra-wideband system capable of concurrent transmission and reception, Part I: requirements and innovations," Proc. Communications, Circuits and Systems Proceedings, 2006.